Diffractive electro- and photo-production of vector mesons in exclusive processes using CGC

Bheemsehan Gurjar

Department of Modern Physics

University of Science and Technology of China, Hefei

Based on : In progress..., PRD 111, 094002 (2025), PRD 109, 094017 (2024)

In collaboration with: A. Kumar (SBU), C. Mondal (IMP, CAS), and S. Kaur (IMP, CAS)

Date : July 14, 2026

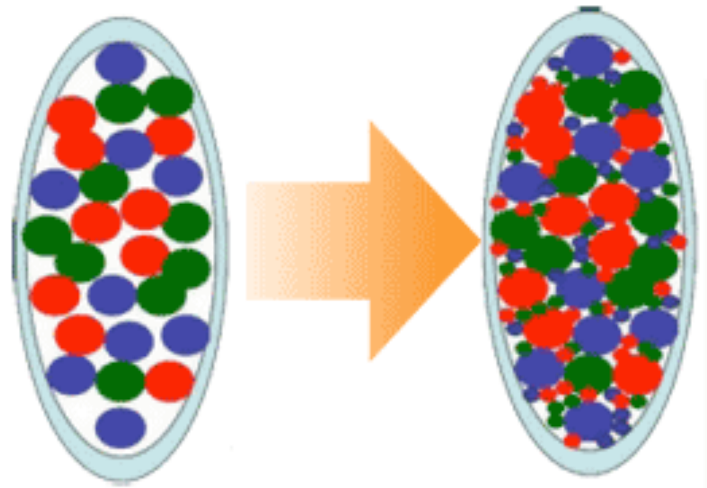

Gluon Saturation, Diffraction and Multi-hadron Production at the EIC, July 14 - 17, 2026 @ CFNS, Stony Brook University, NY, USA.

Outline

- Vector meson production : The CGC dipole model
- Light-Front QCD and hadronic wave functions
  - Photon wave function $\rightarrow$ Light Cone perturbation theory
  - Vector Meson LFWFs $\rightarrow$ Light-Front Holographic QCD
- Diffractive VM production in ep collision at HERA
- Diffractive photoproduction of VM at UPCs
- Conclusion and outlooks

EIC Science Pillars: major ones

◆ Matter forms from fundamental particles through the formation of hadrons, which are composite particles made of quarks.

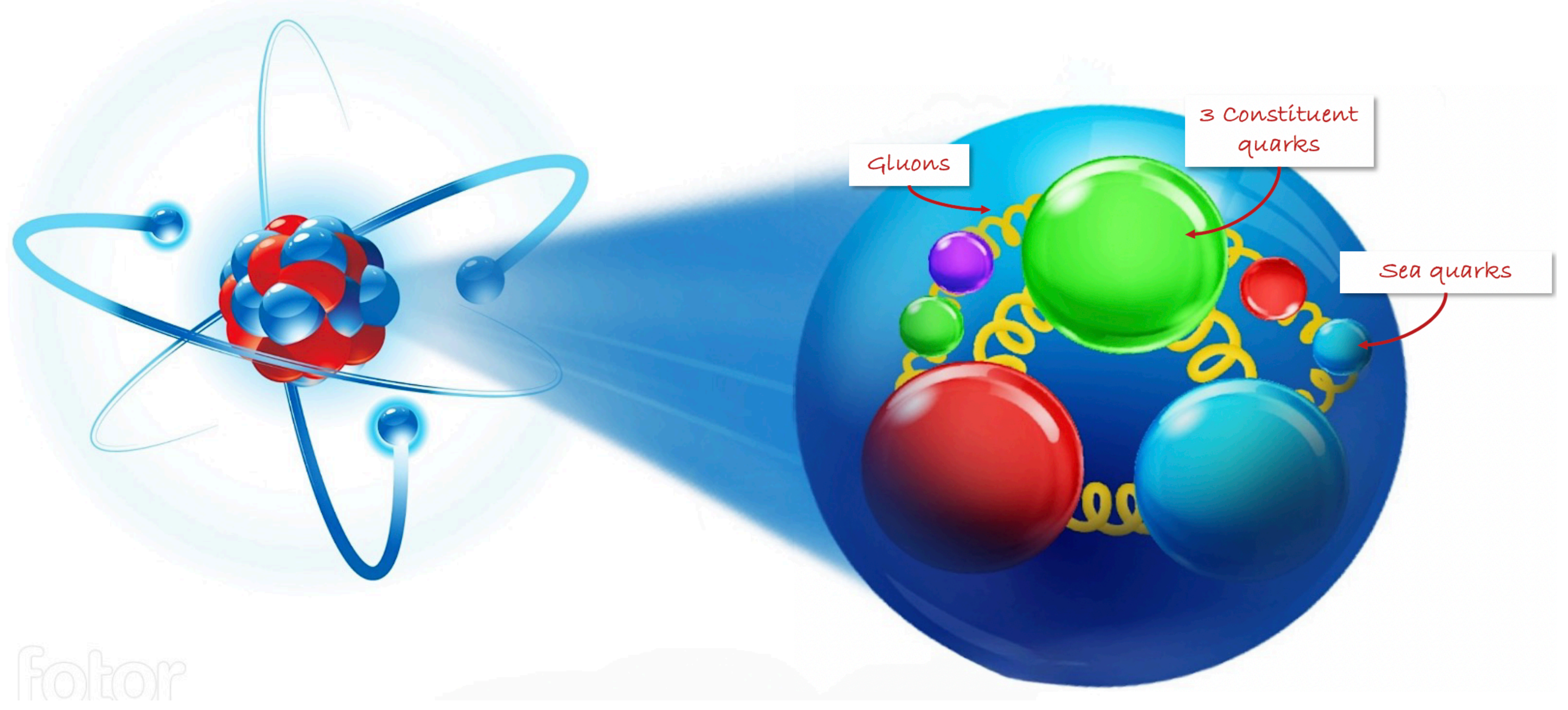

Origin of nucleon mass ?

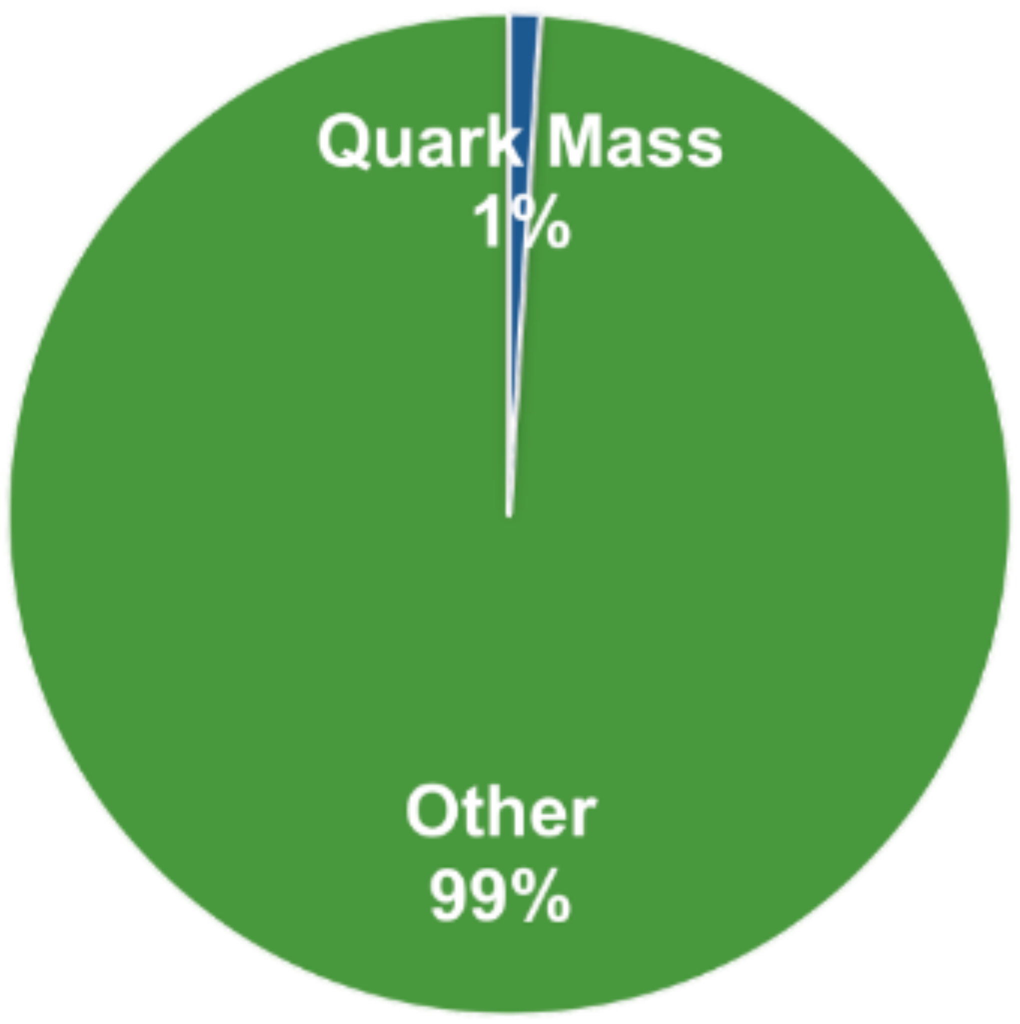

Origin of nucleon spin ?

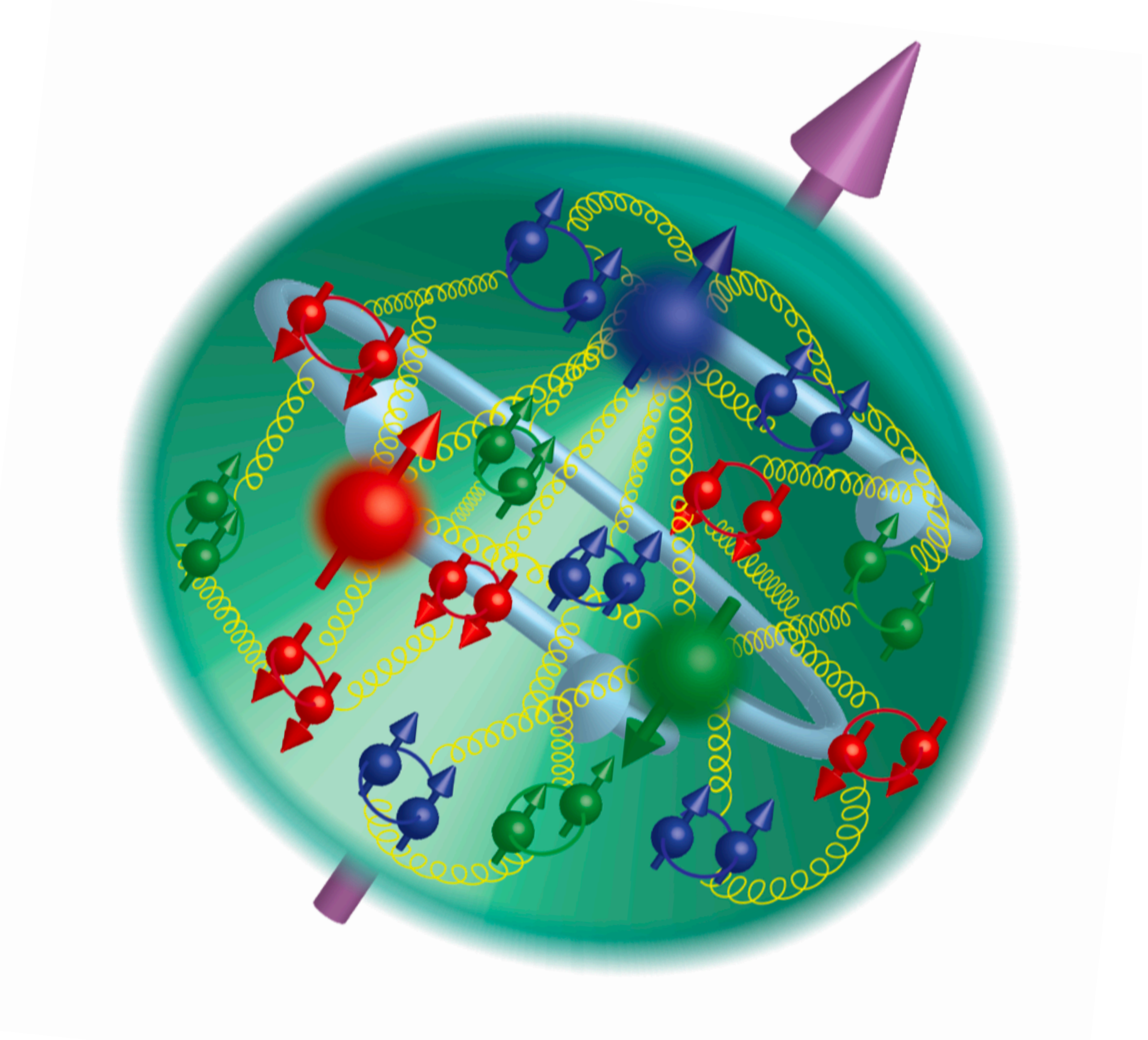

Gluon saturation → CGC ?

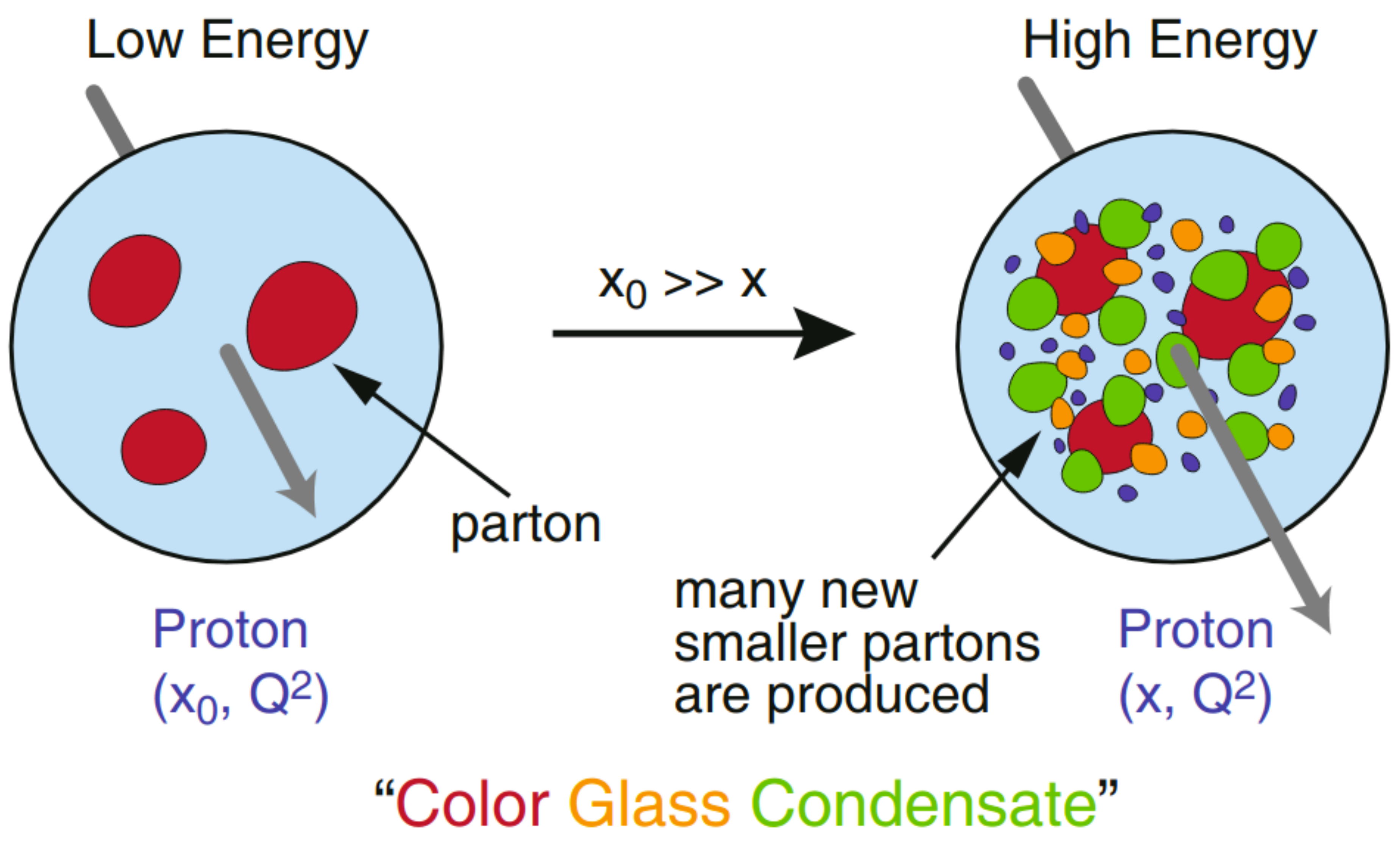

➡ The gluonic dynamics is responsible to address/describe the emergent properties of hadrons.

CGC: Taming Gluon saturation

- Matter forms from fundamental particles through the formation of hadrons, which are composite particles made of quarks.

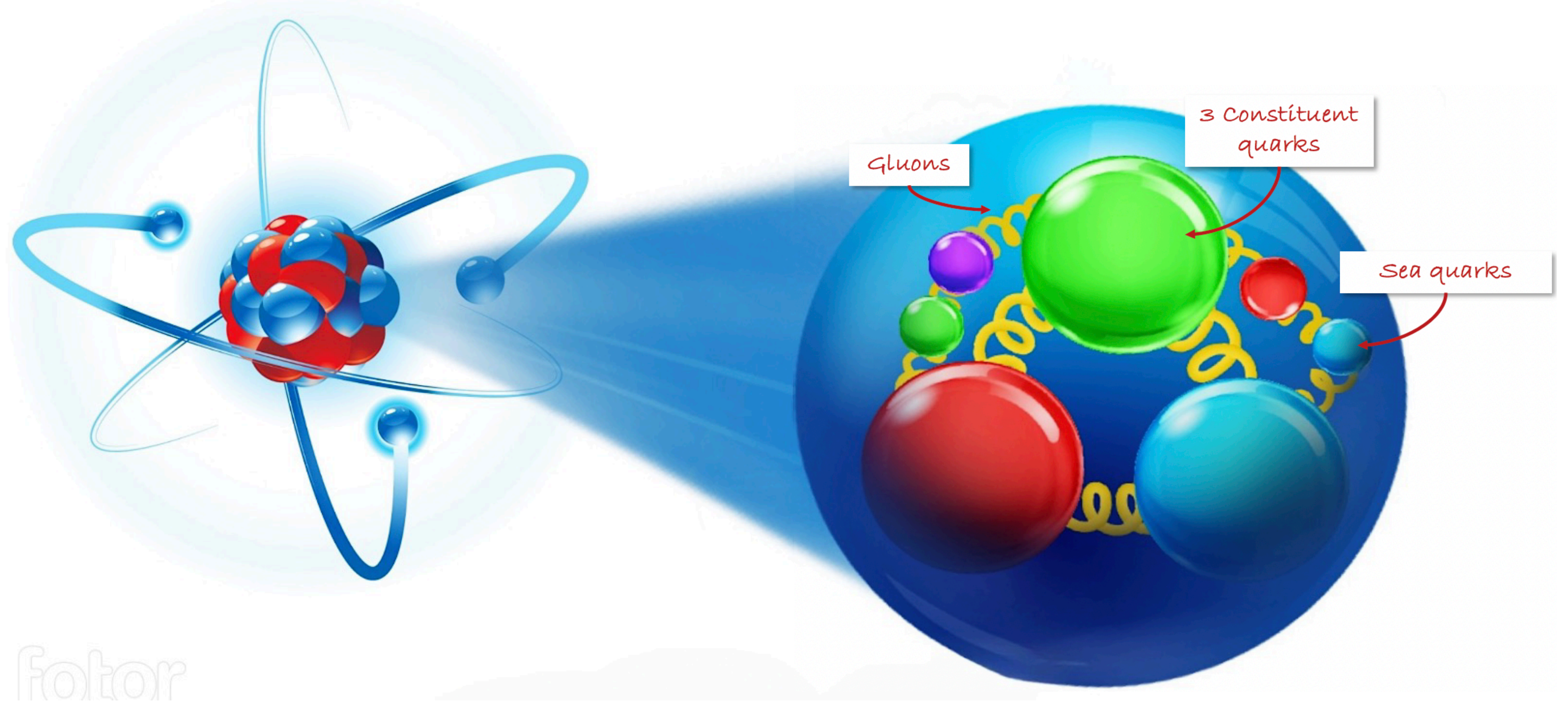

Origin of nucleon mass ?

Origin of nucleon spin ?

Gluon saturation → CGC ?

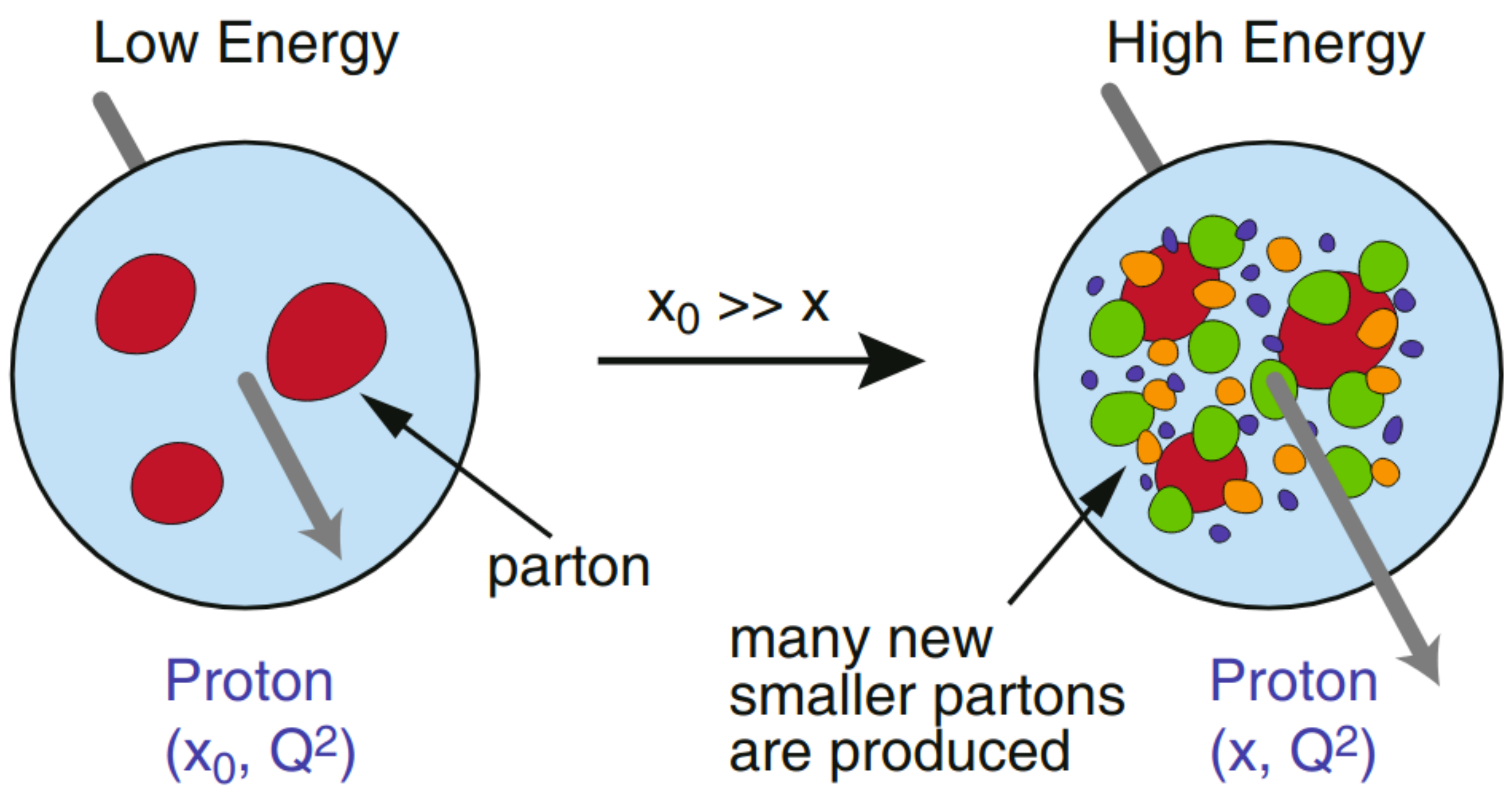

"Color Glass Condensate"

➡The CGC preserves quantum unitarity by balancing gluon splitting with recombination to halt infinite growth.

Gluon Saturation: An unavoidable consequence of QCD

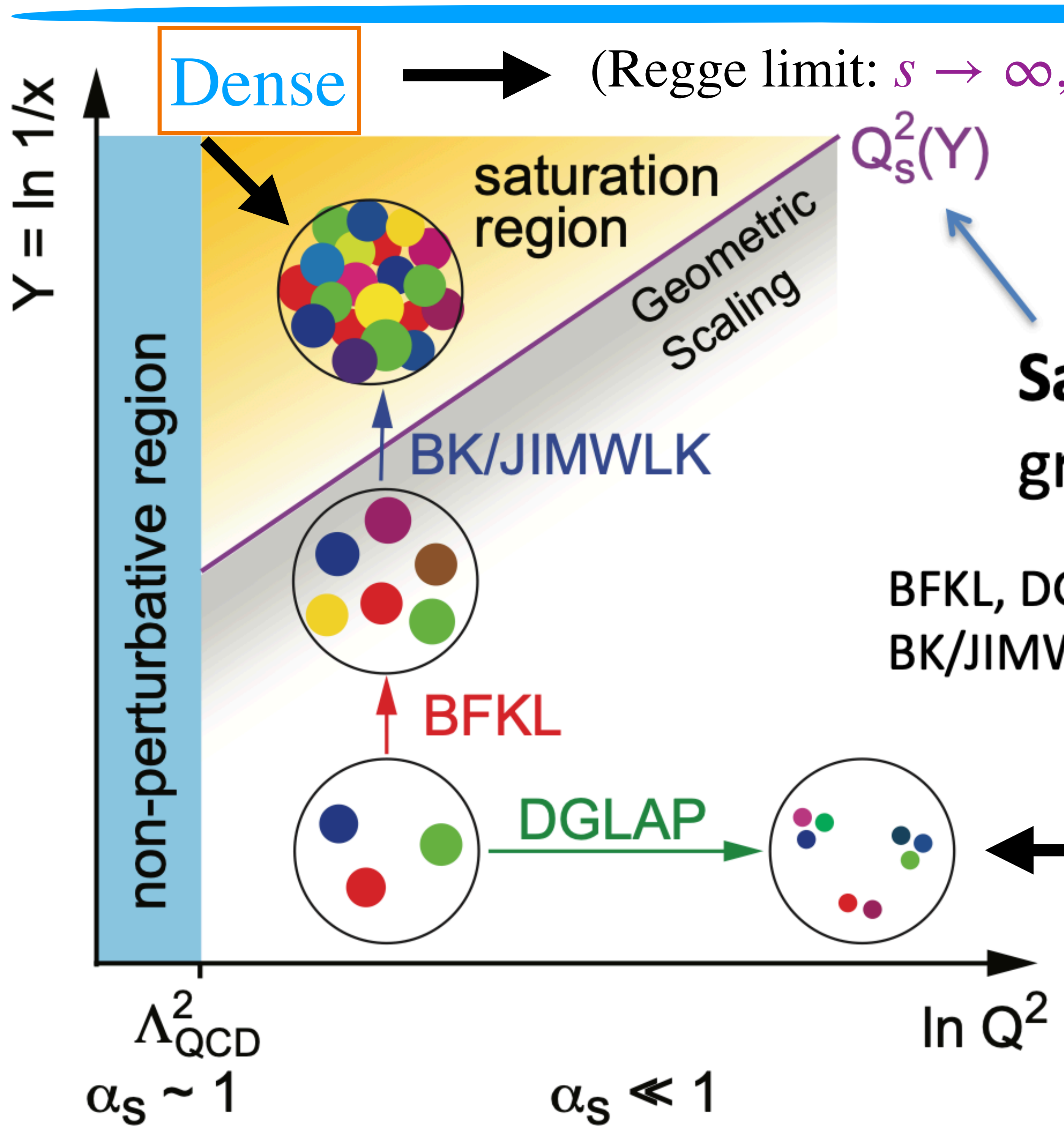

(Regge limit: $s \to \infty$, $x \to 0$, $Q^2 \to$ fixed)

Phase space density increases

Saturation Scale grows with energy

BFKL, DGLAP – linear equations
BK/JIMWLK – nonlinear

Dilute

(Bjorken limit: $s \to \infty$, $Q^2 \to \infty$, $x \to$ fixed)

Phase space density decreases

?

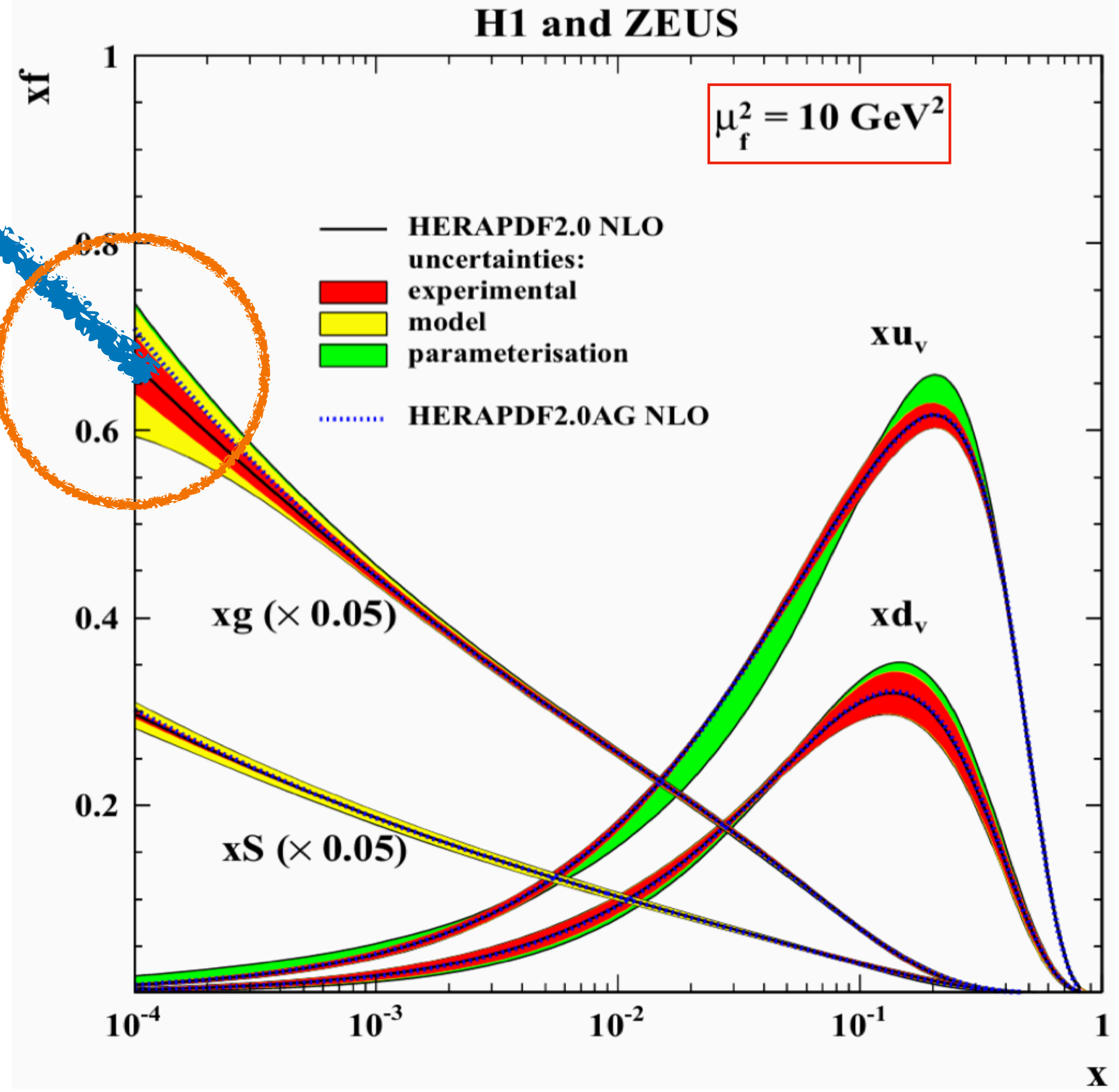

- Gluons dominate nucleon/nucleus structure at small x

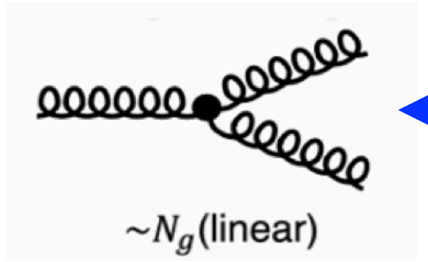

Gluon splitting

- Gluons start to overlap and eventually recombine

Gluon saturation?

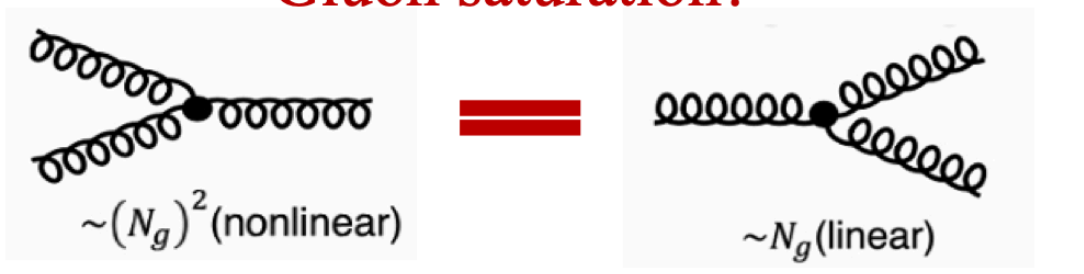

Gluon recombination   Gluon splitting

➡ At small x as gluon density grows rapidly as at high energy: have 1/x singularities → BFKL equation.

➡ At even lower x, gluons will start to recombine which slows down growth: Non-linear dynamics → BK (JIMWLK) equation.

➡ Gluon density will reach a balance, this is called saturation and is defined by the saturation scale $Q_s(x)$.

➡ QCD unitarity: growth of gluon density can't continue indefinitely!

— Iancu, Leonidov, and McLerran, PLB(2001),
— Balitsky and Lipatov, JNP(1978).

$$\frac{\partial N(x,r_T)}{\partial \ln(1/x)} = \alpha_s K_{\mathrm{BFKL}} \otimes N(x,r_T) - \alpha_s [N(x,r_T)]^2.$$

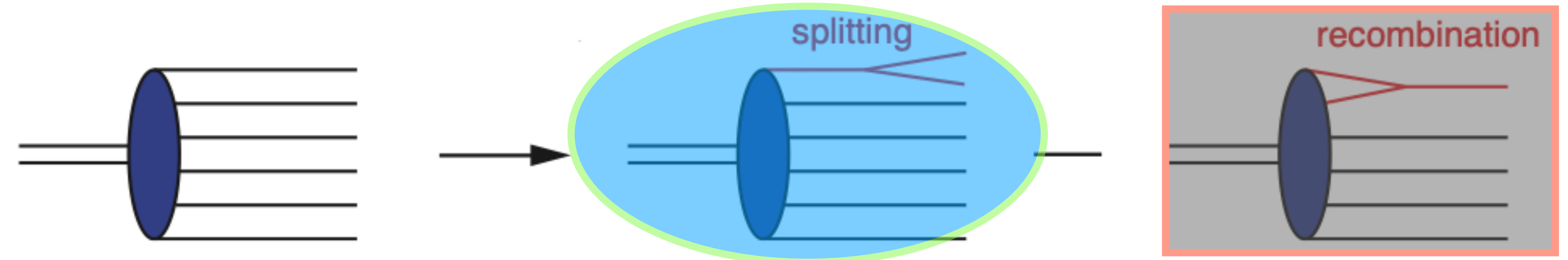

Exclusive VM Production as a Probe of Gluons

➡ Vector meson photoproduction directly probes gluonic structure of nucleus/nucleon.

GPD Picture

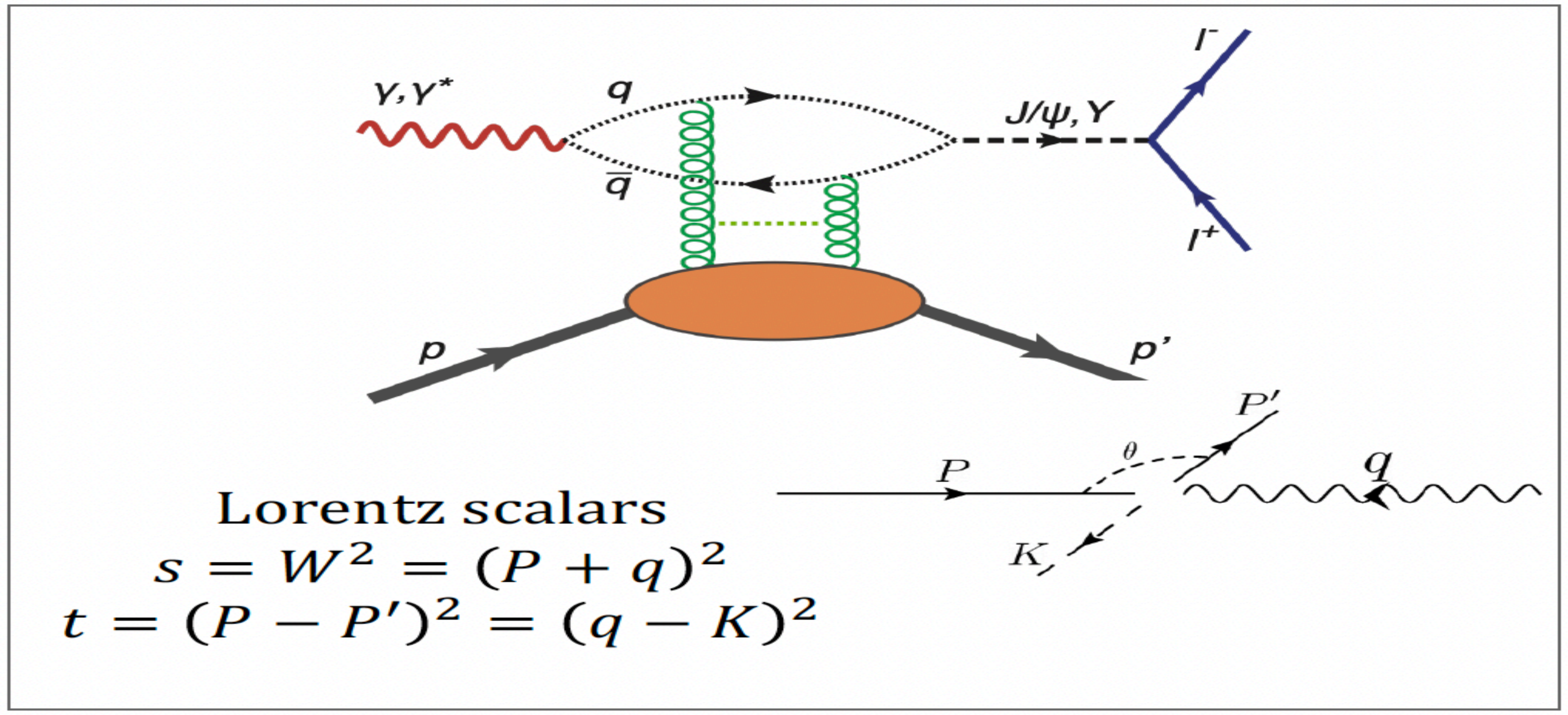

Dominated by color-singlet two-gluon exchange

Dipole Picture

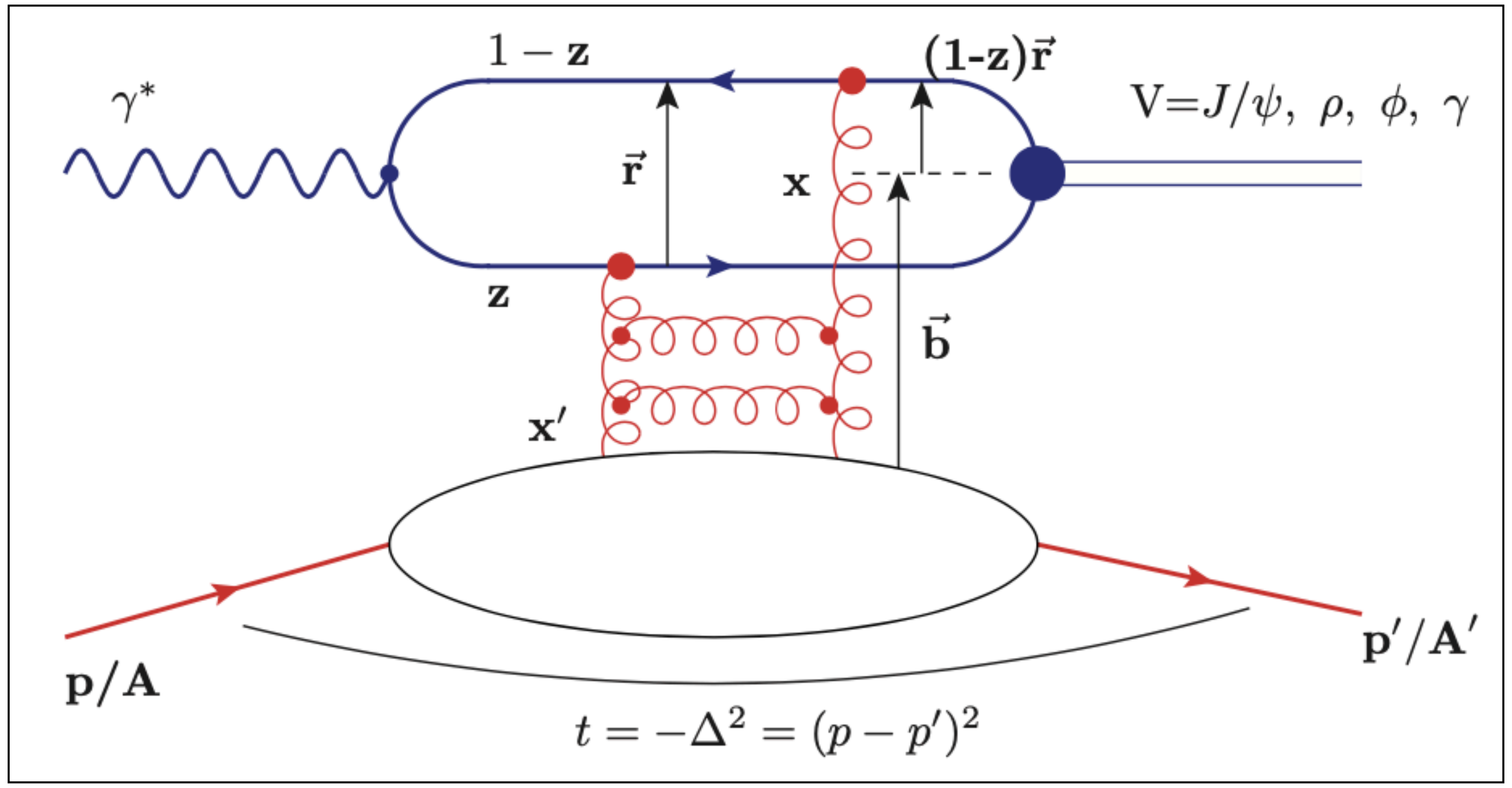

Dominated by multiple-gluon exchange

➡ High energy QCD factorization → The forward scattering amplitude for the diffractive process

$$\mathcal{A}^{\gamma^* p \to Vp} = 2\mathrm{i} \int \mathrm{d}^2\mathbf{b}\,\mathrm{d}^2\mathbf{r} \frac{\mathrm{d}z}{4\pi}\, e^{-i[\mathbf{b}-(\frac{1}{2}-z)\mathbf{r}]\cdot\Delta} \left[\Psi_V^* \Psi_\gamma\right](Q^2, \mathbf{r}, z) N_\Omega(\mathbf{r}, \mathbf{b}, x)$$

– G. Watt and H. Kowalski, PRD 78, (2008), E. Iancu, et al. B 590, 199(2004)

- High energy factorization:
  - $\gamma^* \to q\bar{q}$ splitting, wavefunction $\Psi_\gamma(Q^2, \mathbf{r}, z)$
  - Elastic scattering of $q\bar{q}$ dipole: $N_\Omega(\mathbf{r}, \mathbf{b}, x)$
  - $q\bar{q} \to J/\Psi$, wavefunction $\Psi_V(\mathbf{r}, z)$

➡ The virtual photon and VM WFs can be obtained within Light-Front quantizations framework.

Light-Front Quantization

➡ Hamiltonian field theory on the light front is identified as one of the natural frameworks to describe hadron structure and QCD.

	instant form	**front form**	**point form**
time variable	$t = x^0$	$x^+ \triangleq x^0 + x^3$	$\tau \triangleq \sqrt{t^2 - \vec{x}^2 - a^2}$
quantization surface	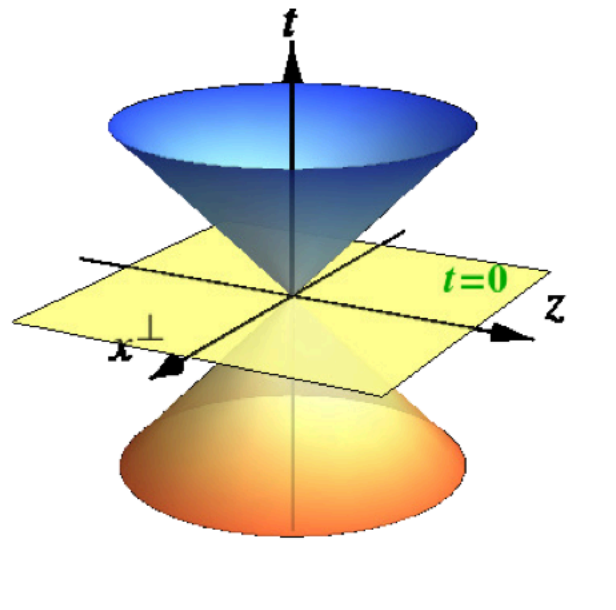		
Hamiltonian	$H = P^0$	$P^- \triangleq P^0 - P^3$	P^μ
kinematical	$\vec{P}, \vec{J}$	$\vec{P}^\perp, P^+, \vec{E}^\perp, E^+, J_z$	$\vec{J}, \vec{K}$
dynamical	$\vec{K}, P^0$	$\vec{F}^\perp, P^-$	$\vec{P}, P^0$
dispersion relation	$p^0 = \sqrt{\vec{p}^2 + m^2}$	$p^- = (\vec{p}_\perp^2 + m^2)/p^+$	$p^\mu = m v^\mu \ (v^2 = 1)$

$$O \sim \langle \Psi | \hat{O} | \Psi \rangle$$

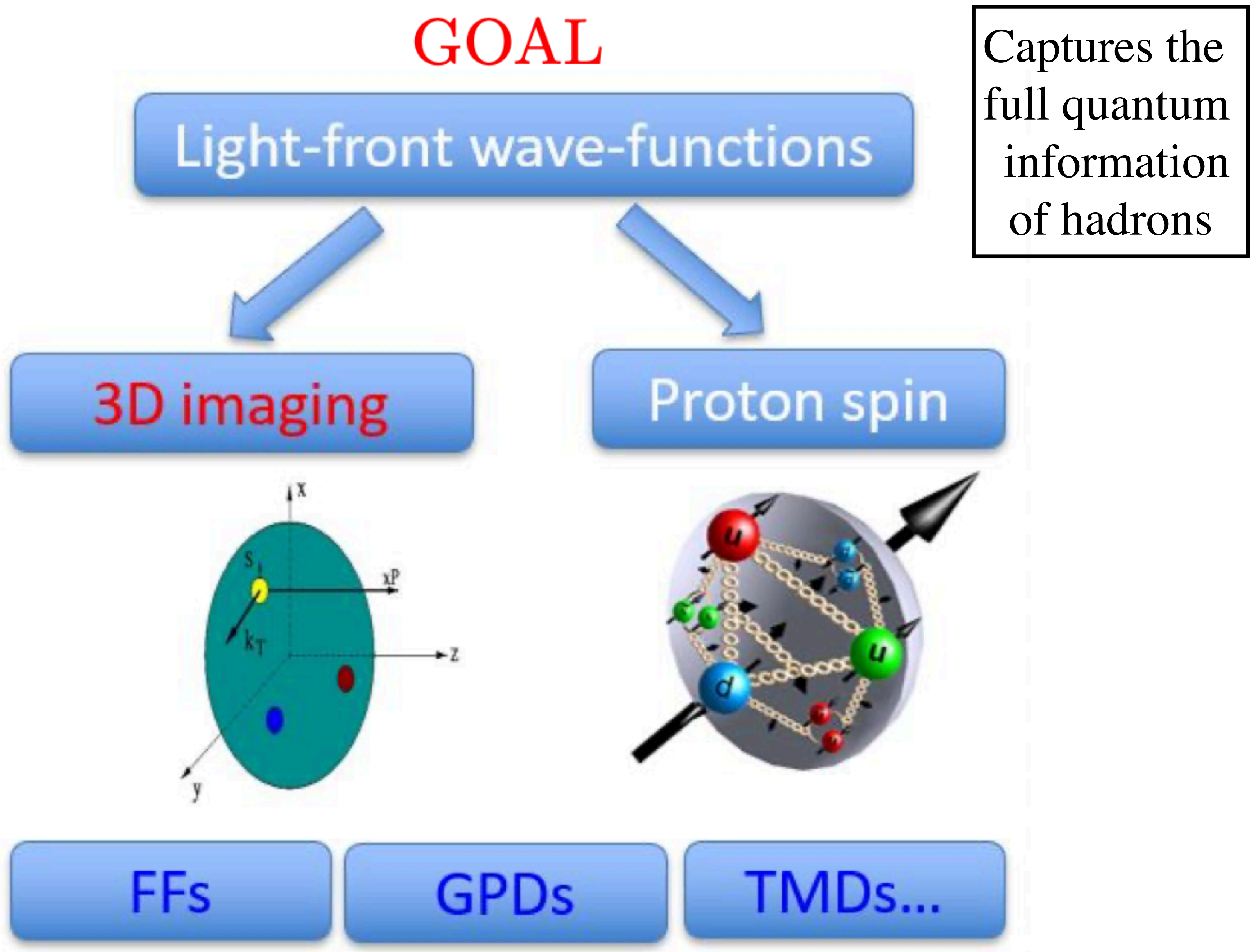

➡ Relativistic light-front Schrodinger-like equation :

$$i \frac{\partial}{\partial x^+} |\psi(x^+)\rangle = \frac{1}{2} \underline{P}^- |\psi(x^+)\rangle \quad \Rightarrow \quad \underline{H}_{\text{LFQCD}} |\psi_h(P, j, m_j)\rangle = M_h^2 |\psi_h(P, j, m_j)\rangle \longrightarrow$$

Direct access to partonic observables in Minkowski spacetime

$$\boxed{\underline{H}_{\text{LFQCD}} = P^+ \underline{P}^-_{\text{LFQCD}} - \vec{P}_\perp^2}$$

➡

Mass spectra → Eigen value
Eigen modes → Boost invariance/frame independence LFWFs

—Dirac, Rev.Mod.Phys. (1949), Brodsky, Pauli, Pinsky, Phys.Rept.(1998)

Light-Front Wave functions

Photon LFWFs : LF QED

- The photon light-front wavefunctions can be computed perturbatively in QED.

$$\Psi^{\gamma,L}_{h,\bar{h}}(r,x;Q^2,m_f) = \sqrt{\frac{N_c}{4\pi}}\delta_{h,-\bar{h}}\, e\, e_f\, 2x(1-x)Q\frac{K_0(\epsilon r)}{2\pi}\,,$$

$$\Psi^{\gamma,T}_{h,\bar{h}}(r,x;Q^2,m_f) = \pm\sqrt{\frac{N_c}{2\pi}}\, e\, e_f\left[ie^{\pm i\theta_r}(x\delta_{h\pm,\bar{h}\mp}-(1-x)\delta_{h\mp,\bar{h}\pm})\partial_r + m_f\delta_{h\pm,\bar{h}\pm}\right]\frac{K_0(\epsilon r)}{2\pi}$$

Where $\epsilon^2 = x(1-x)Q^2 + m_f^2$

In $Q \to 0$ or $x \to (0,1)$ limit : m_f acts as infrared regulator.

— G. P. Lepage and S. J. Brodsky PRD22 (1980)

Meson LFWFs : LF Holographic QCD

- The longitudinal and transversely polarized vector meson light-front wave functions :

$$\Psi^{V,L}_{h,\bar{h}}(r,x) = \frac{1}{2}\delta_{h,-\bar{h}}\left[1+\frac{m_f^2-\nabla_r^2}{x(1-x)M_V^2}\right]\Psi\ (r,x)\,.$$

$$\Psi^{V,T}_{h,\bar{h}}(r,x) = \pm\left[ie^{\pm i\theta_r}(x\delta_{h\pm,\bar{h}\mp}-(1-x)\delta_{h\mp,\bar{h}\pm})\partial_r + m_f\delta_{h\pm,\bar{h}\pm}\right]\frac{\Psi\ (r,x)}{2x(1-x)}\,.$$

— J. R. Forshaw and R. Sandapen, PRL109 (2012)

Light-Front Holographic QCD (LFHQCD)

Light-front Schrödinger wave equation with a factorization ansatz

$$\begin{aligned} ds^2 &= g_{MN}dx^M dx^N \\ &= \frac{R^2}{z^2}\left(\eta_{\mu\nu}dx^\mu dx^\nu - dz^2\right) \end{aligned} \quad \Rightarrow \quad S = \frac{1}{2}\int d^dx\, dz\, \sqrt{g}\, e^{\varphi(z)}\left(g^{MN}\partial_M\Phi\partial_N\Phi - \mu^2\Phi^2\right)$$

$$\left(\frac{\vec{k}_\perp^2 + m_q^2}{x} + \frac{\vec{k}_\perp^2 + m_{\bar{q}}^2}{1-x} + U\right)\psi(x,\vec{k}_\perp) = M^2\psi(x,\vec{k}_\perp)$$

factorization ansatz $\Downarrow$ $\psi = \varphi(\vec{\zeta}_\perp)\chi(x)$

$$\left[-\nabla^2_{\zeta_\perp} + U_\perp(\vec{\zeta}_\perp)\right]\varphi(\vec{\zeta}_\perp) = M_\perp^2\varphi(\vec{\zeta}_\perp), \quad \left[\frac{\cancel{m_q^2}}{x} + \frac{\cancel{m_{\bar{q}}^2}}{1-x} + U_\parallel(\tilde{z})\right]\chi(x) = M_\parallel^2\chi(x)$$

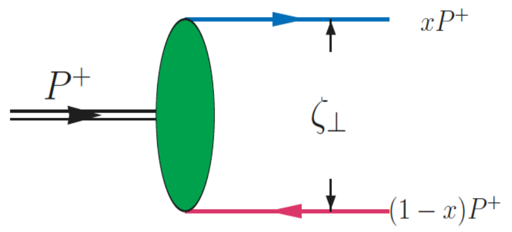

semiclassical LFQCD	$\leftrightarrow$	semiclassical field theory in AdS
$\zeta_\perp = \sqrt{x(1-x)}r_\perp$	$\leftrightarrow$	fifth coordinate z,
LF amplitude	$\leftrightarrow$	string amplitude
confining potential	$\leftrightarrow$	dilation field Φ
$L^2-(J-2)^2$	$\leftrightarrow$	$(\mu R)^2$
Form factors	$\leftrightarrow$	form factors

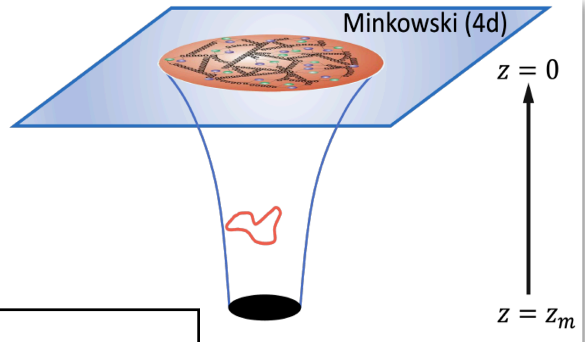

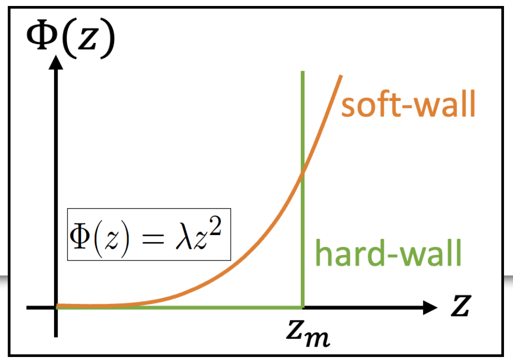

Breaking of the conformal symmetry by the dilaton field

- Transverse mode : Can obtained by solving the LF Schrödinger equation

$$\left(-\frac{d^2}{d\zeta^2} - \frac{1-4L^2}{4\zeta^2} + U_\perp(\zeta)\right)\phi(\zeta) = M_\perp^2\phi(\zeta);$$

with $U_\perp(\zeta) = \kappa^4\zeta^2 + 2\kappa^2(J-1)$ and $\zeta = \sqrt{x(1-x)}r_\perp$.

$$\Psi(x,\zeta) = \frac{\kappa}{\sqrt{\pi}}\sqrt{x(1-x)}\exp\left[-\frac{\kappa^2\zeta^2}{2}\right].$$

- Longitudinal mode : 't Hooft equation which can be derived by using the QCD lagrangian in (1+1) dimension with large N_c approximations :

$$\left(\frac{m_q^2}{x} + \frac{m_{\bar{q}}^2}{1-x}\right)\chi(x) + \frac{g^2}{\pi}\mathcal{P}\int dy\frac{\chi(x)-\chi(y)}{(x-y)^2} = M_\parallel^2\chi(x);$$

Using the matrix method $\Rightarrow$ $\chi(x) \simeq x^{\beta_1}(1-x)^{\beta_2}$, with

$\beta_1 = (3m_q^2/\pi g^2)^{1/2}$, and $\beta_2 = (3m_{\bar{q}}^2/\pi g^2)^{1/2}$

- Total Holographic vector meson light-front wavefunction :

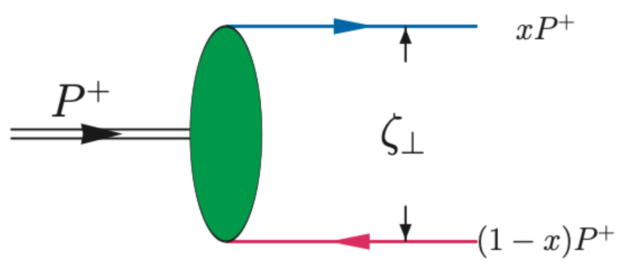

$$\Psi_\lambda(x,\zeta) = \mathcal{N}_\lambda\sqrt{x(1-x)}x^{\beta_1}(1-x)^{\beta_2}\exp\left[-\frac{\kappa^2\zeta^2}{2}\right]$$

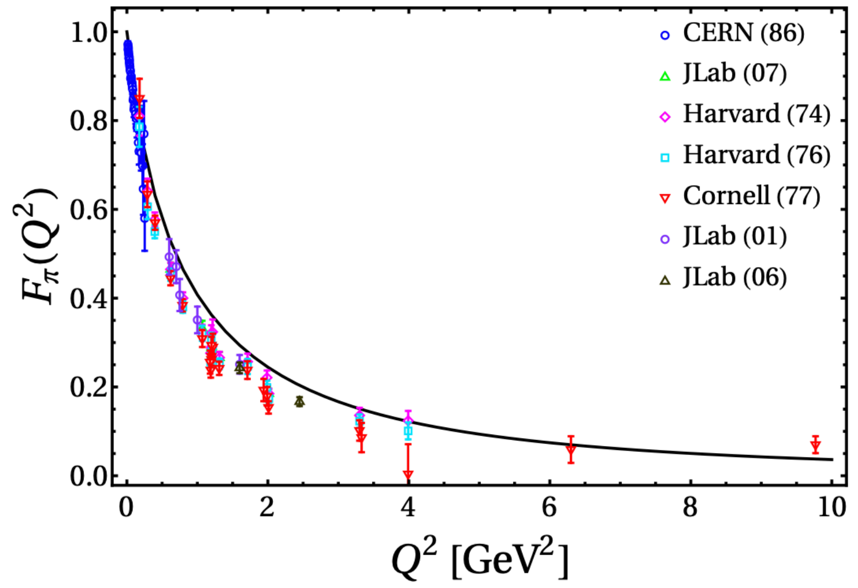

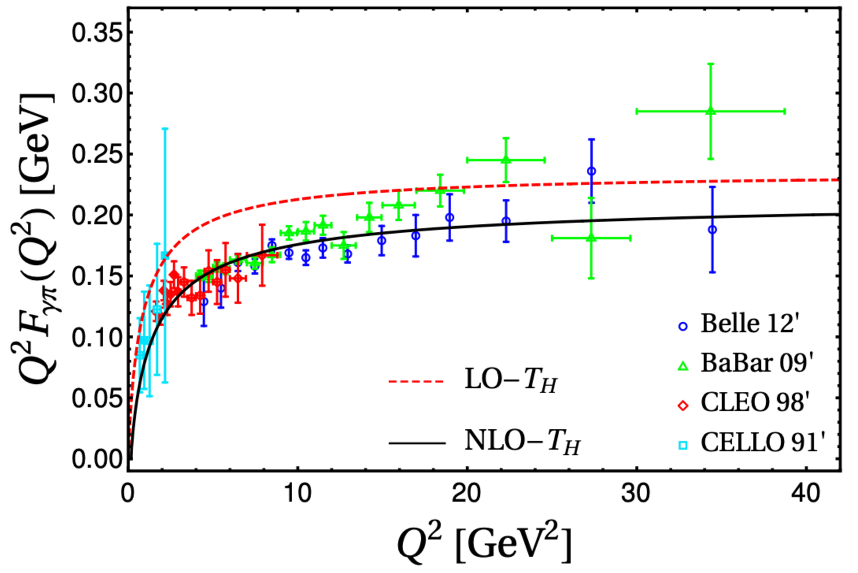

— Teramond, S.J. Brodsky PRD, 104 (2021), C. Mondal et al. PLB, 823 (2021), J.R. Hiller, Ann. Phys. 337 (2013), G. 't Hooft, NPB 75 (1974).

b-CGC Dipole model *vs* IP Sat model

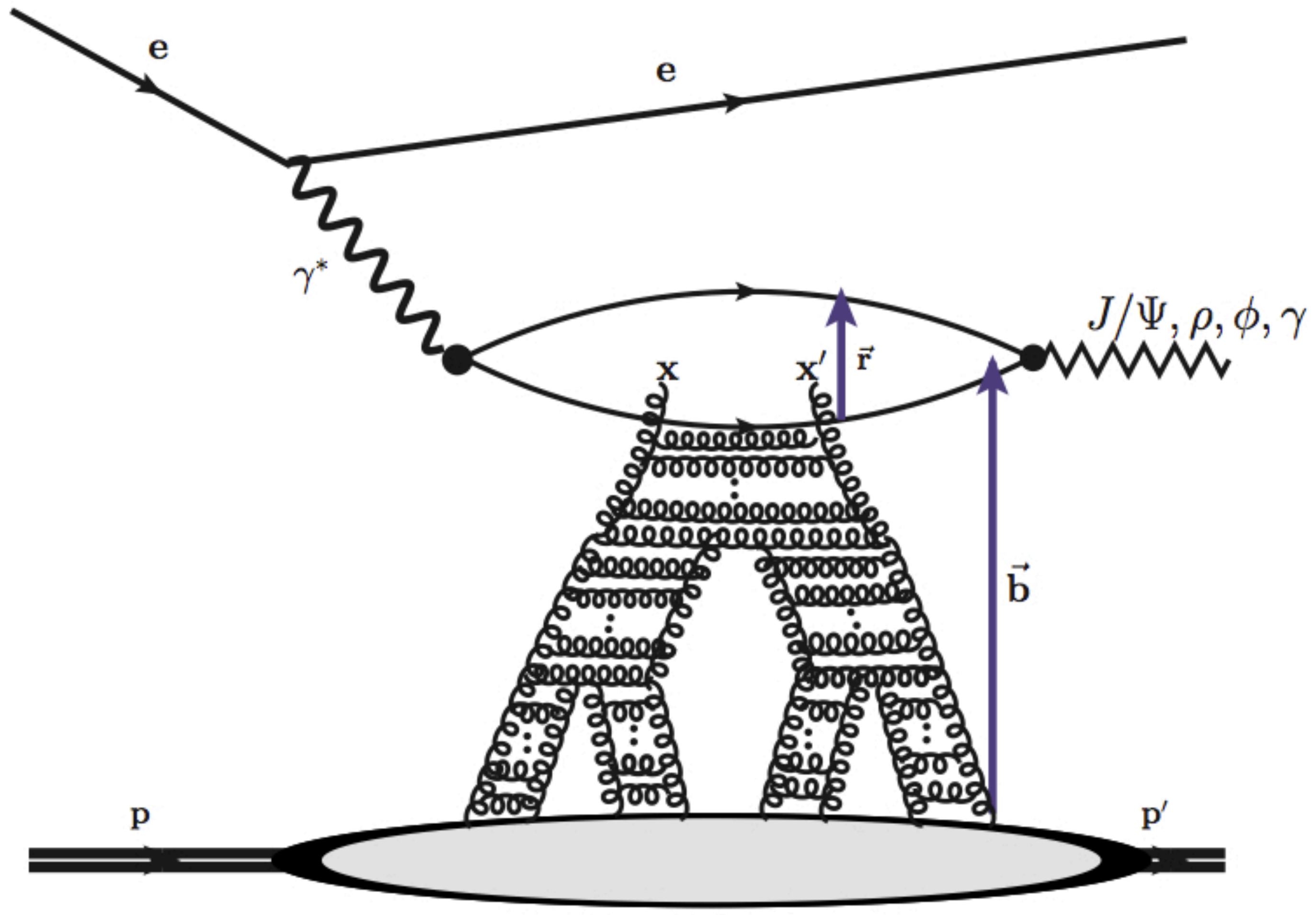

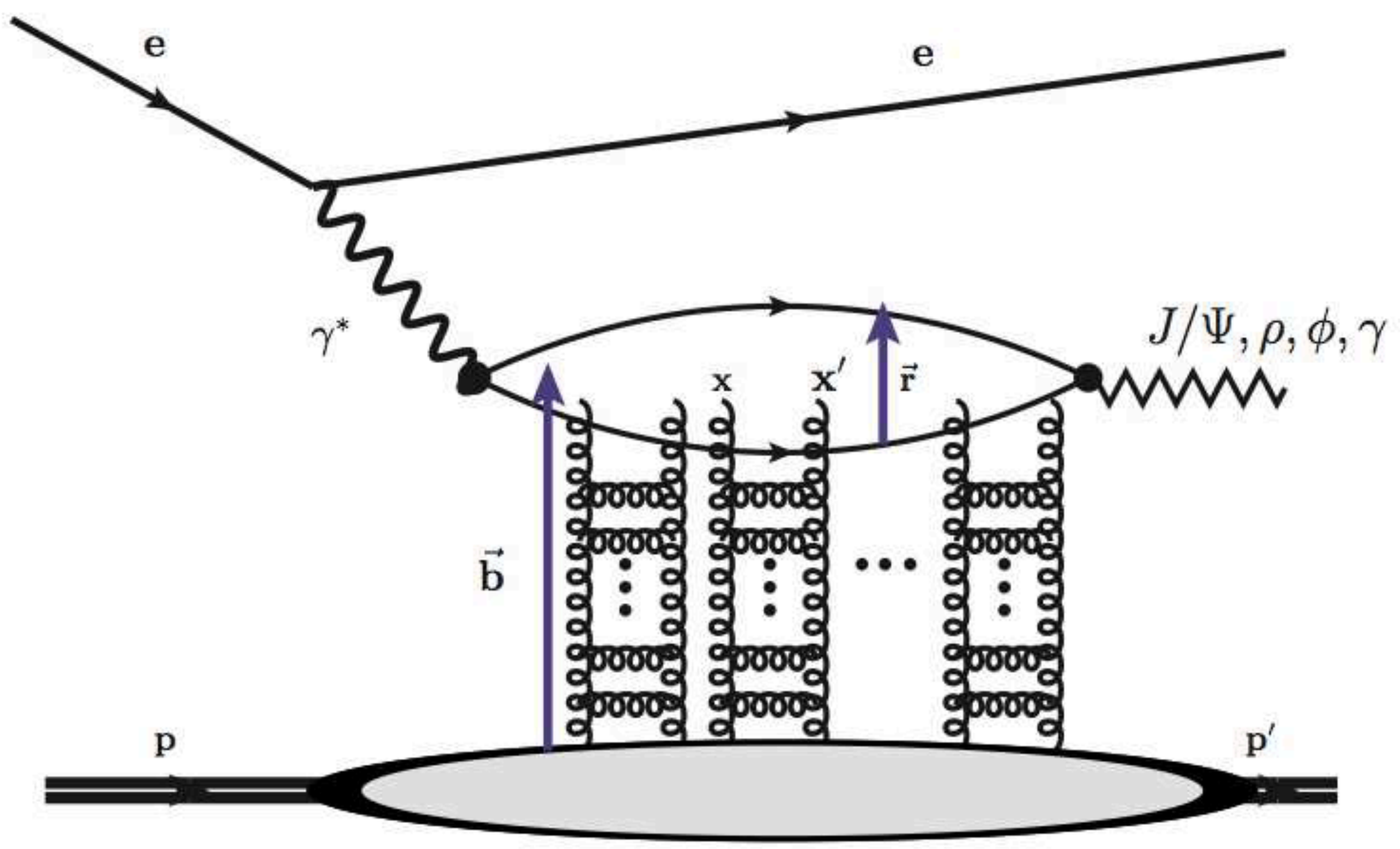

➡ Approximate solution of the Balitsky-Kovchegov equation

$$\mathcal{N}^p(x,\boldsymbol{r},\boldsymbol{b}) = \begin{cases} \mathcal{N}_0 \left(\frac{r\,Q_s(b)}{2}\right)^{2\left(\gamma_s + \frac{\ln(2/r\,Q_s(b))}{\kappa\,\lambda\,y}\right)} & r\,Q_s(b) \le 2 \\ 1 - e^{-A\,\ln^2(B\,r\,Q_s(b))} & r\,Q_s(b) > 2\,, \end{cases}$$

➡ The saturation scale $\rightarrow$ $Q_s(b)$

$$Q_s(x,b) = \left(\frac{x_0}{x}\right)^{\frac{\lambda}{2}} \left[\exp\left(-\frac{b^2}{2B_{\rm CGC}}\right)\right]^{\frac{1}{2\gamma_s}},$$

$[m_{u,d}, m_s]$ GeV	$[m_c]$ GeV	λ	γ_s	σ_0/mb	x_0	χ^2/d.o.f
[0.14, 0.14]	1.27	0.206	0.724	29.9	6.33×10^{-6}	1.07

➡ Eikonalized DGLAP-evolved gluon density with Gaussian b-dependence (Glauber-Mueller amplitude):

$$\mathcal{N}^p(x,\boldsymbol{r},\boldsymbol{b}) = 1 - \exp\left[\frac{\pi^2 r^2}{N_c}\alpha_s(\mu^2)\, xg\left(x, \frac{4}{r^2}+\mu_0^2\right)\, T_G(b)\right],$$

➡ With a Gaussian profile

$$T_G(b) = \frac{1}{2\pi B_G}\exp\left(-\frac{b^2}{2B_G}\right).$$

gluon distribution evolved via DGLAP equation,

initial gluon distribution

$$\boxed{xg\left(x,\mu_0^2\right) = A_g\, x^{-\lambda_g}(1-x)^{5.6}}$$

— Watt, Kowalski, Phys.Rev.D 78 (2008), Rezaeian, Schmidt Phys.Rev.D 88 (2013), Kowalski, Teaney, Kowalski, Phys.Rev.D 68 (2003), Motyka, Watt, Phys.Rev.D 74 (2006)

Model predictions for ρ - meson diffractive production

➡ W-dependence of Total diffractive cross section for $\gamma^* p \to \rho p$ in different Q^2 bins and compared with HERA data.

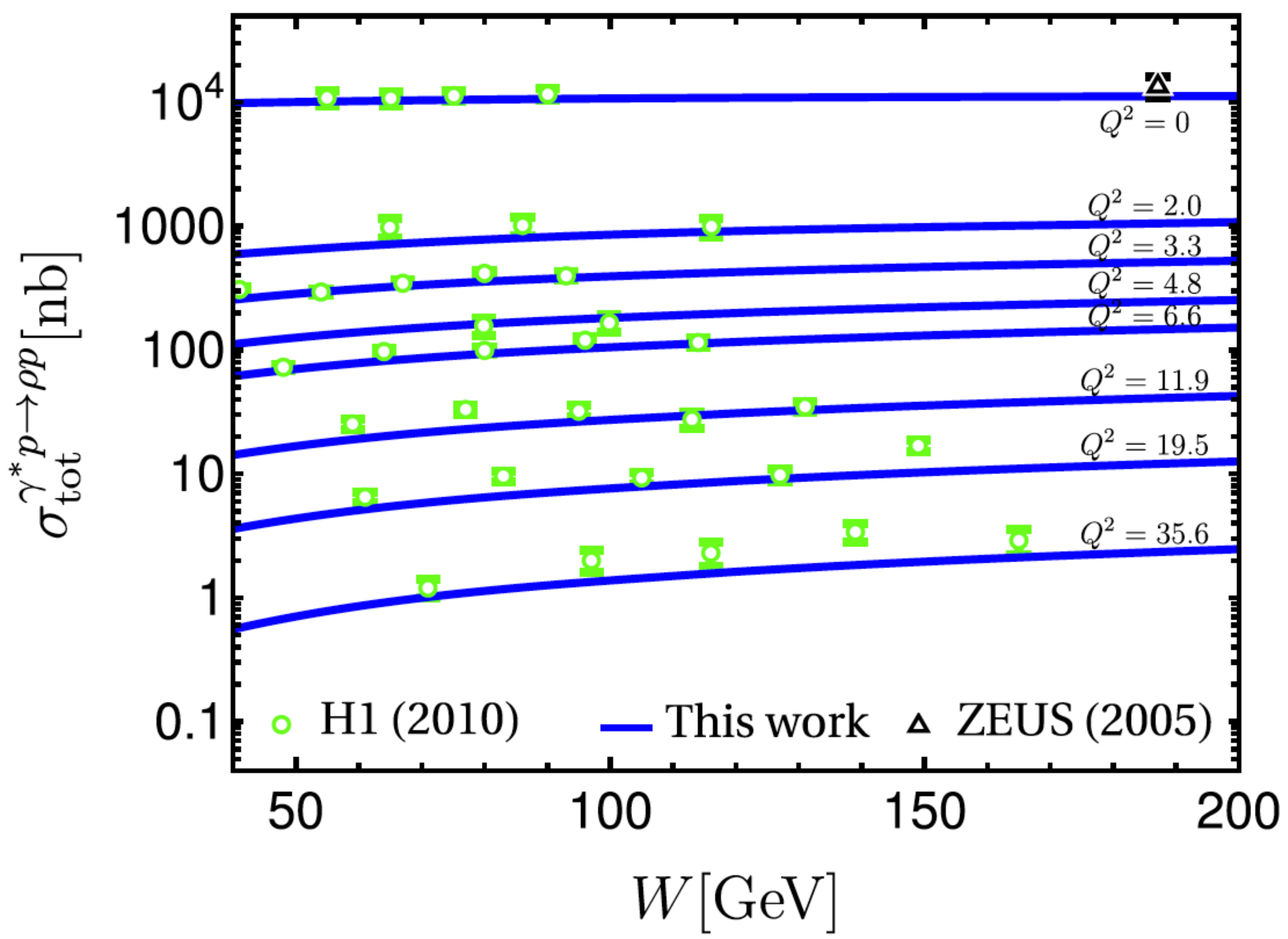

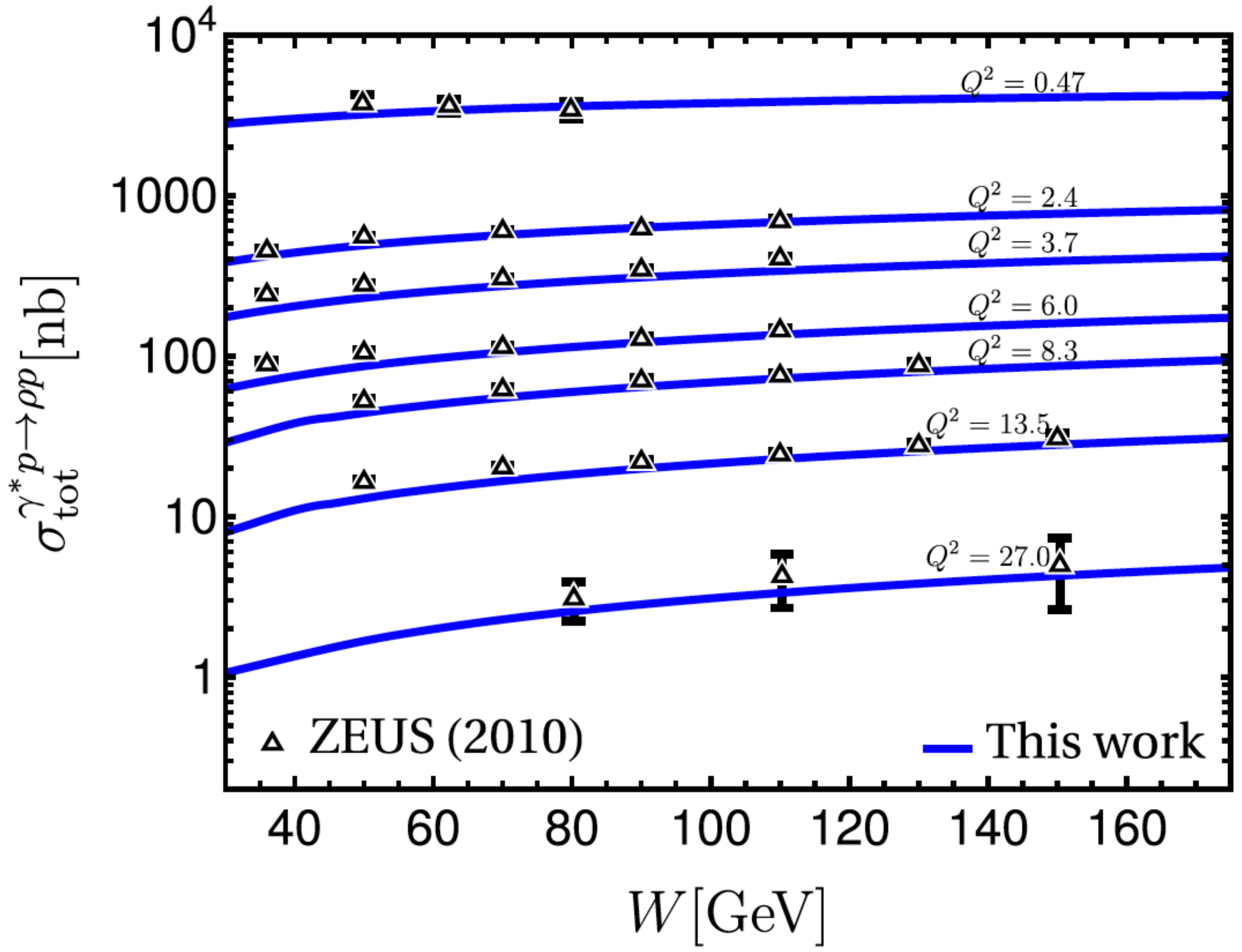

$$\sigma_{\rm tot}^{\gamma^* p \to Vp}(x, Q^2) = \sigma_{\Lambda=\pm 1}^{\gamma^* p \to Vp}(x, Q^2) + \varepsilon \sigma_{\Lambda=0}^{\gamma^* p \to Vp}(x, Q^2)$$

- The HLFQCD predictions along with `t Hooft wf are consistent with HERA data.

—BG, C. Mondal, S. Kaur, Phys.Rev.D 109 (2024)

➡ $|t|$-dependence of Differential and Q^2-dependence of Total diffractive cross section for $\gamma^* p \to \rho p$ compared with HERA data.

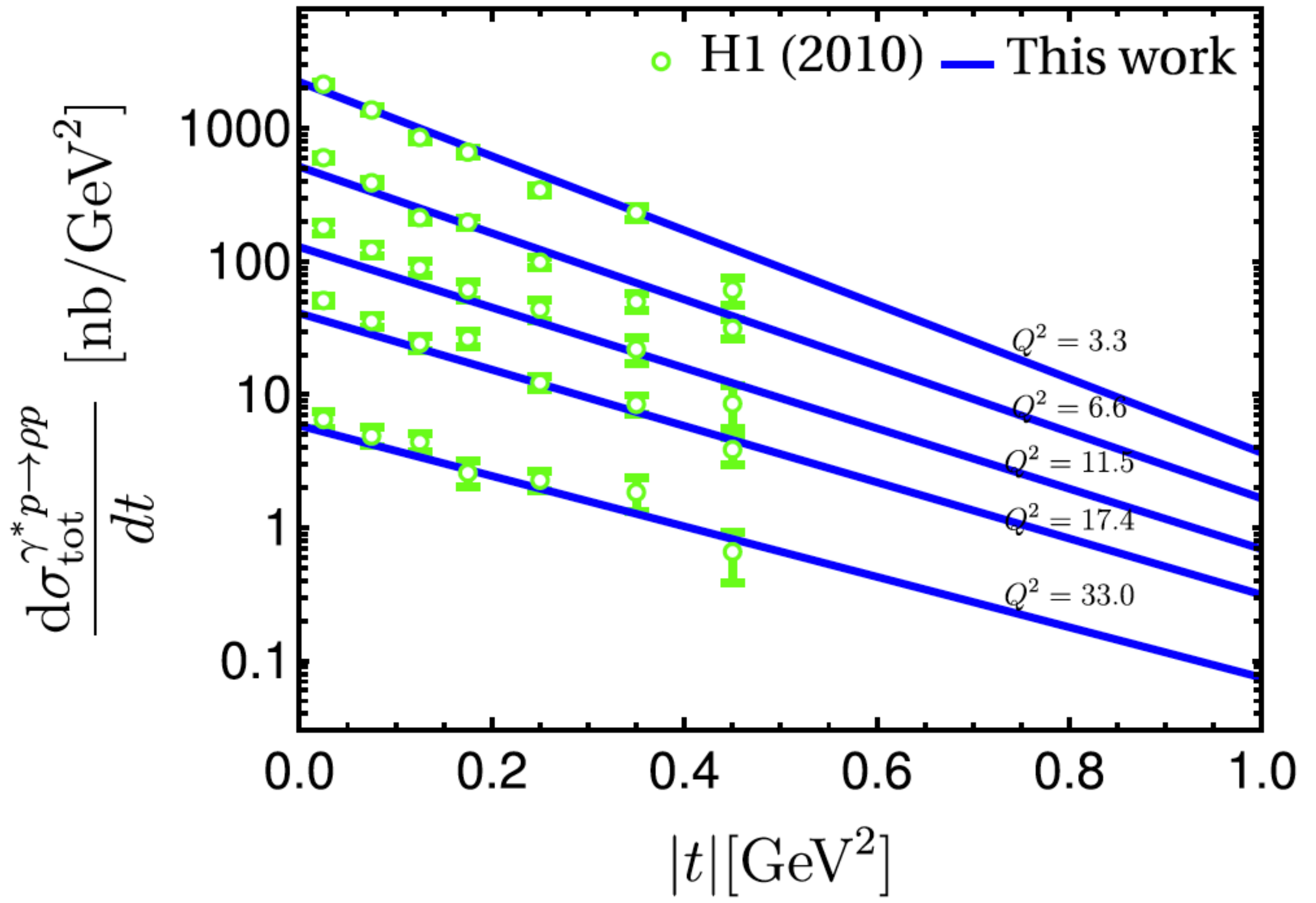

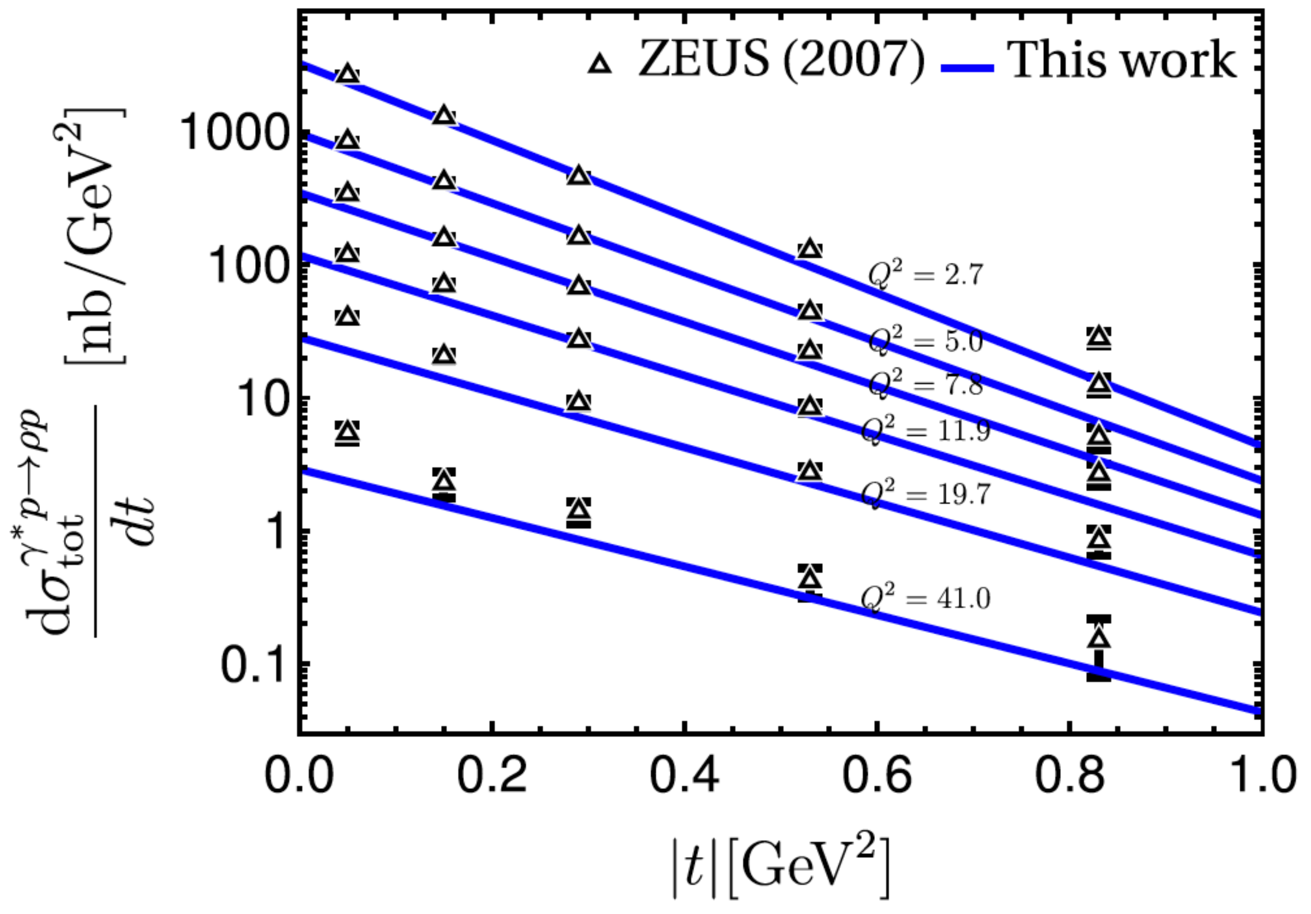

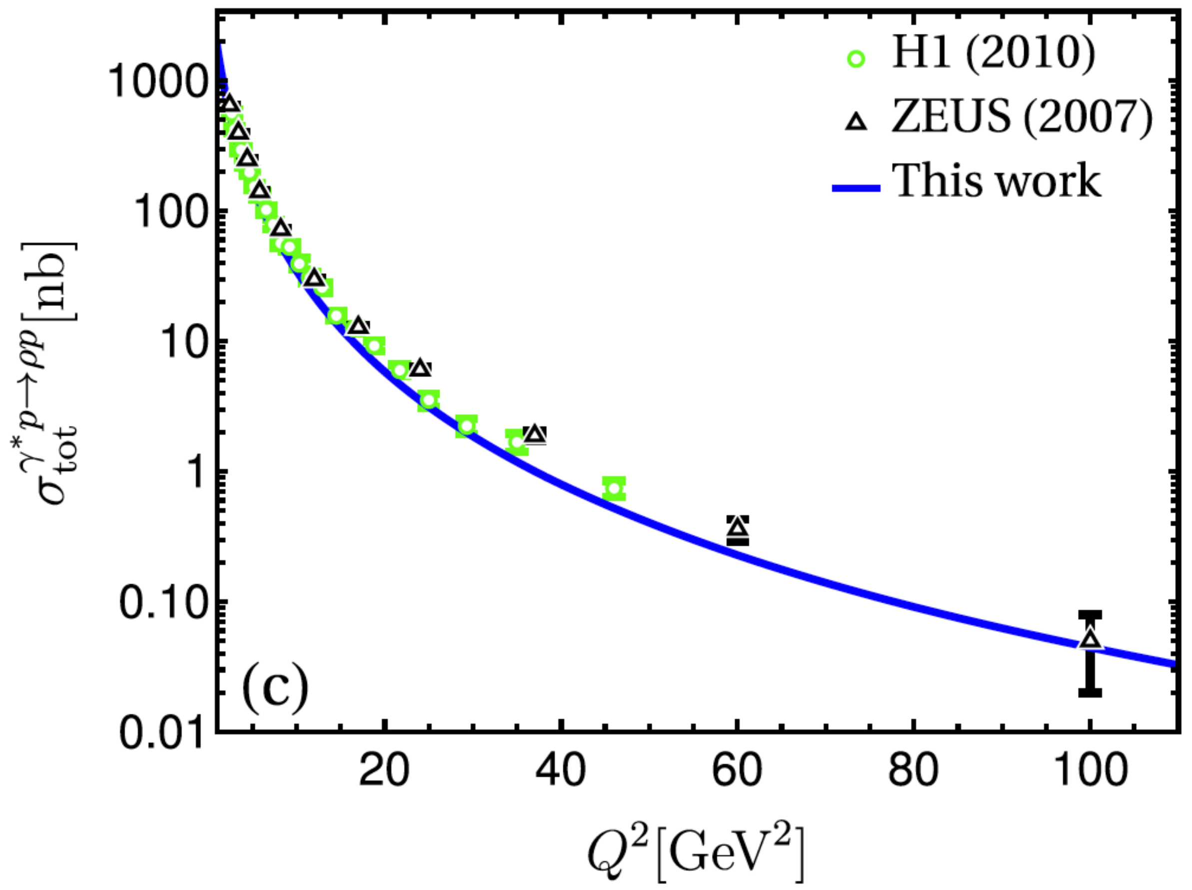

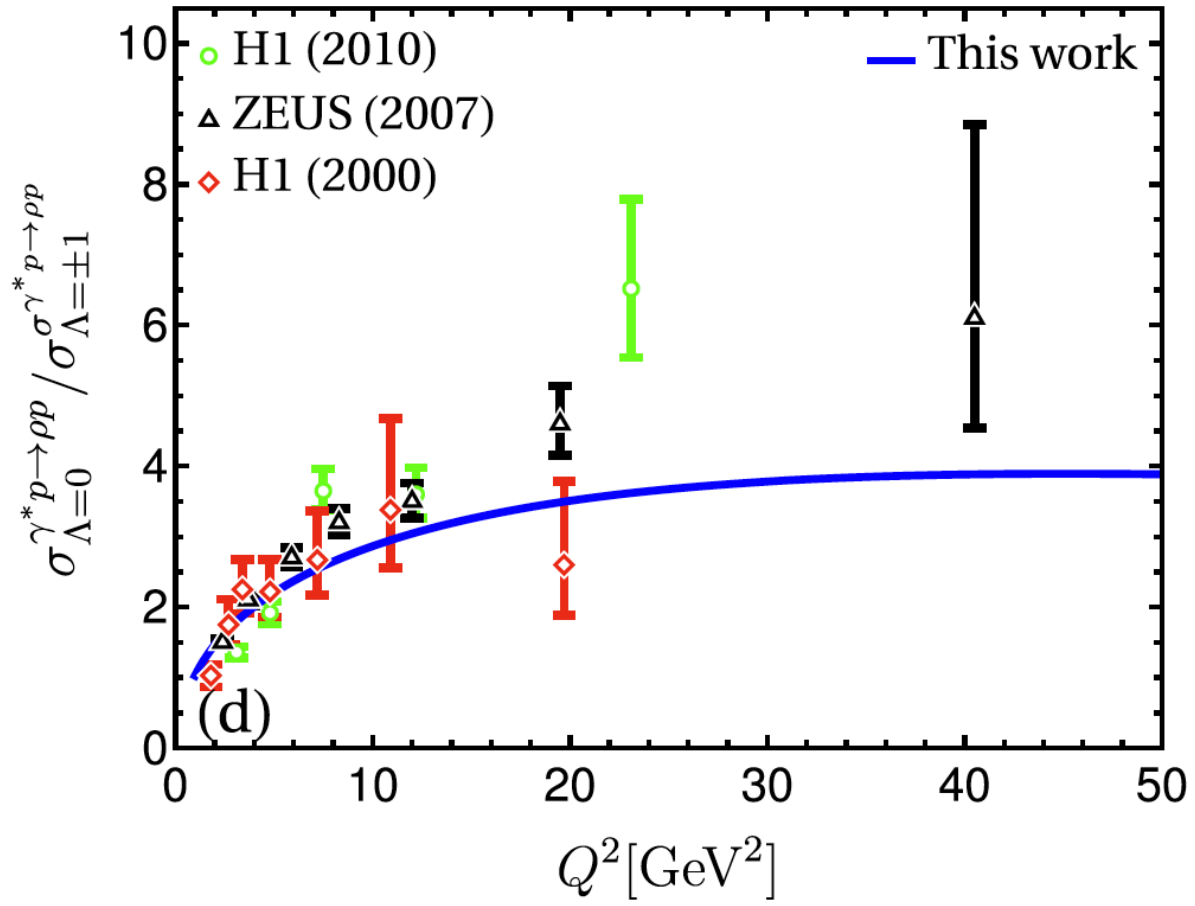

ϕ - meson diffractive production

➡ W-dependence of Total and $|t|$-dependence of Differential for $\gamma^* p \to \phi p$ diffractive cross section in different Q^2 bins and compared with HERA data.

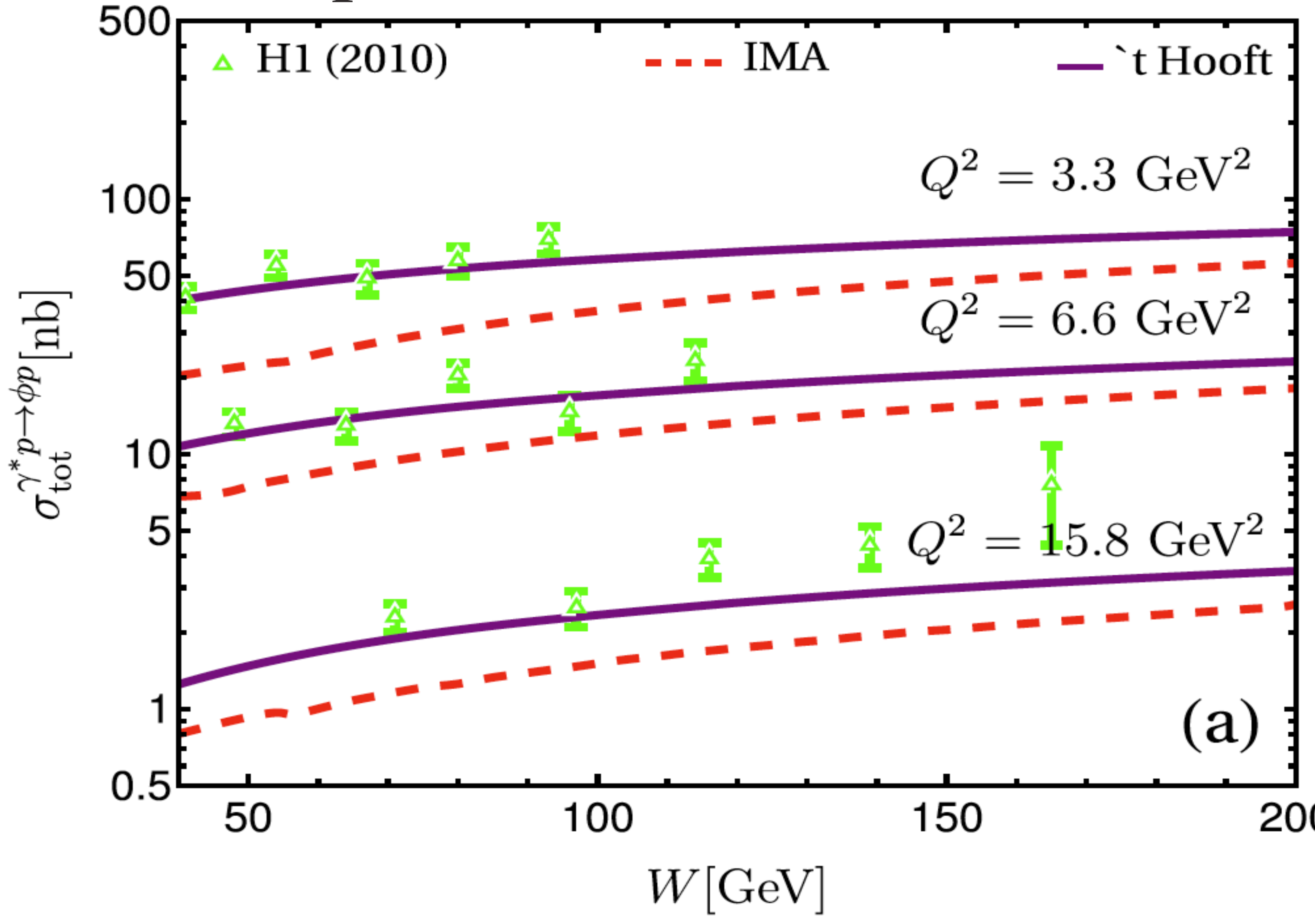

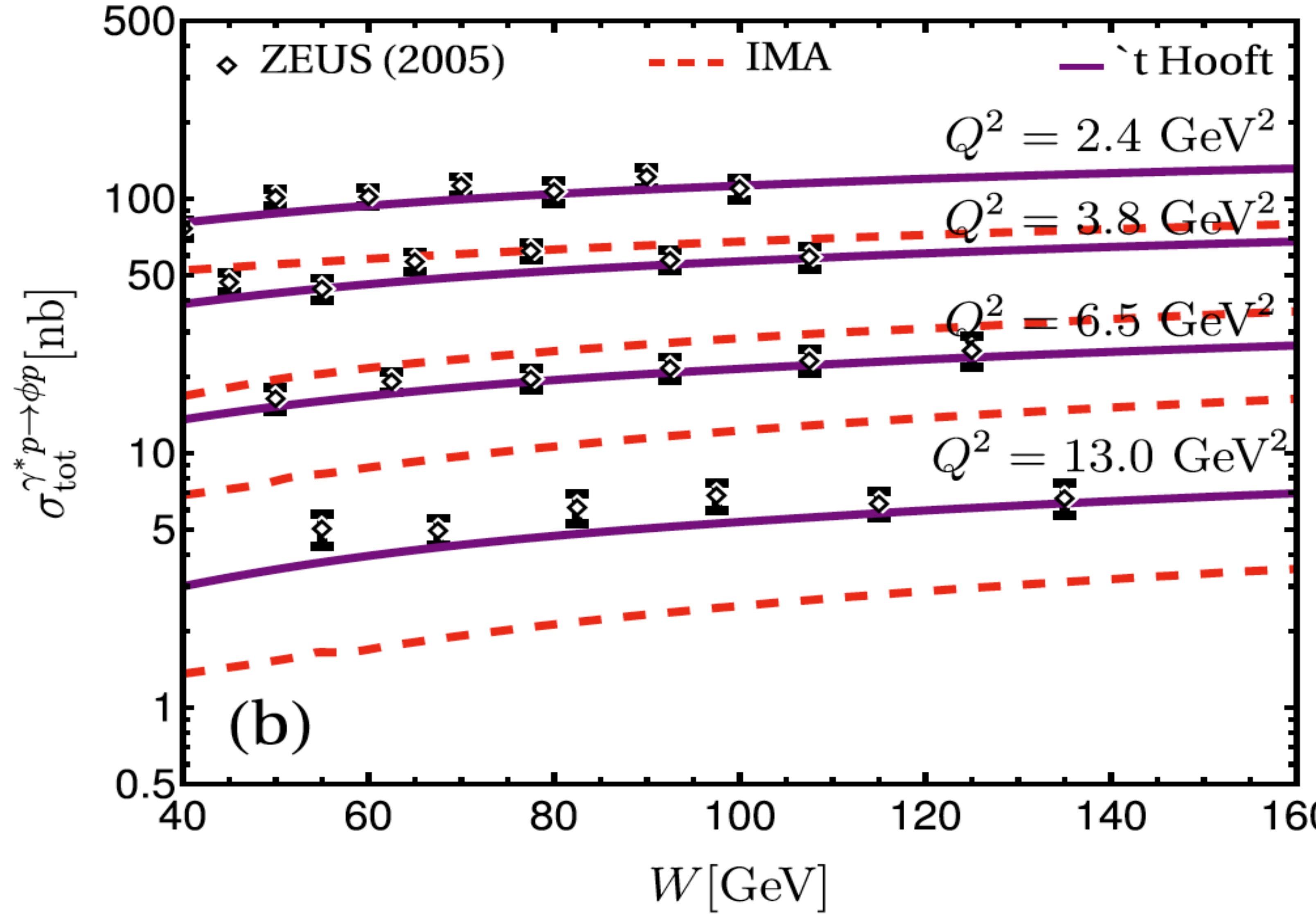

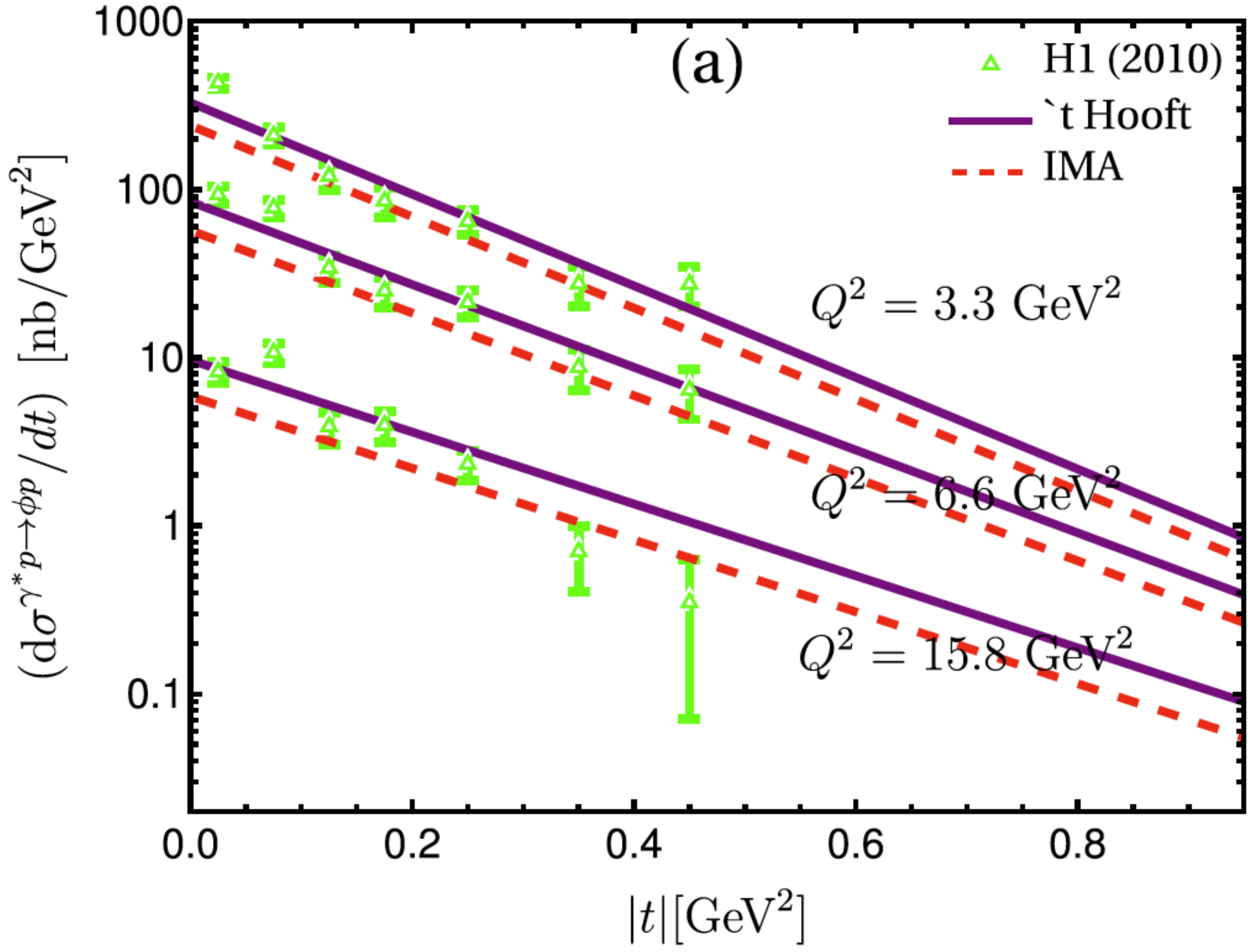

➡ Q^2-dependence of Total and the ration between ϕ and ρ diffractive cross section for $\gamma^* p \to \phi p$ compared with HERA data.

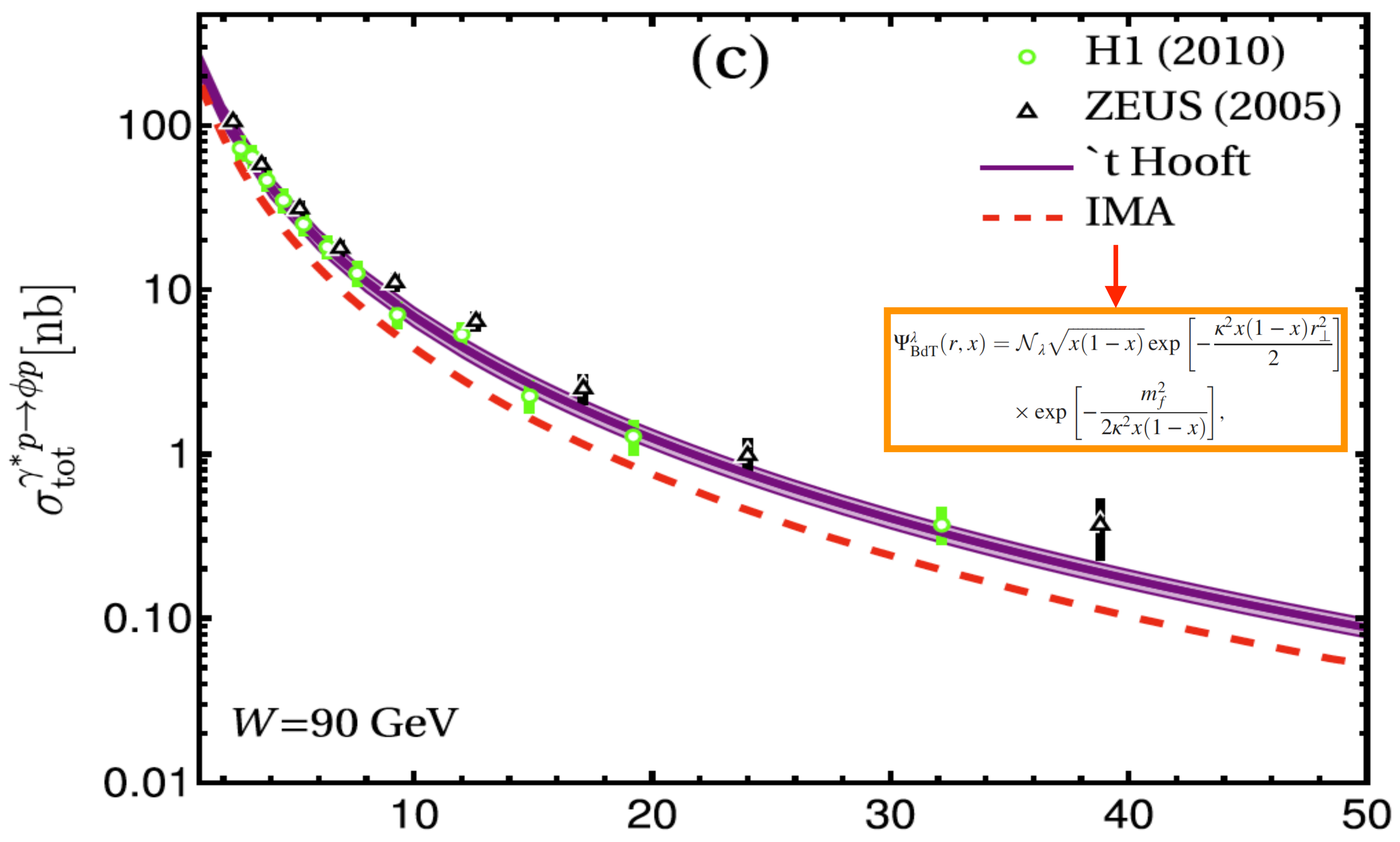

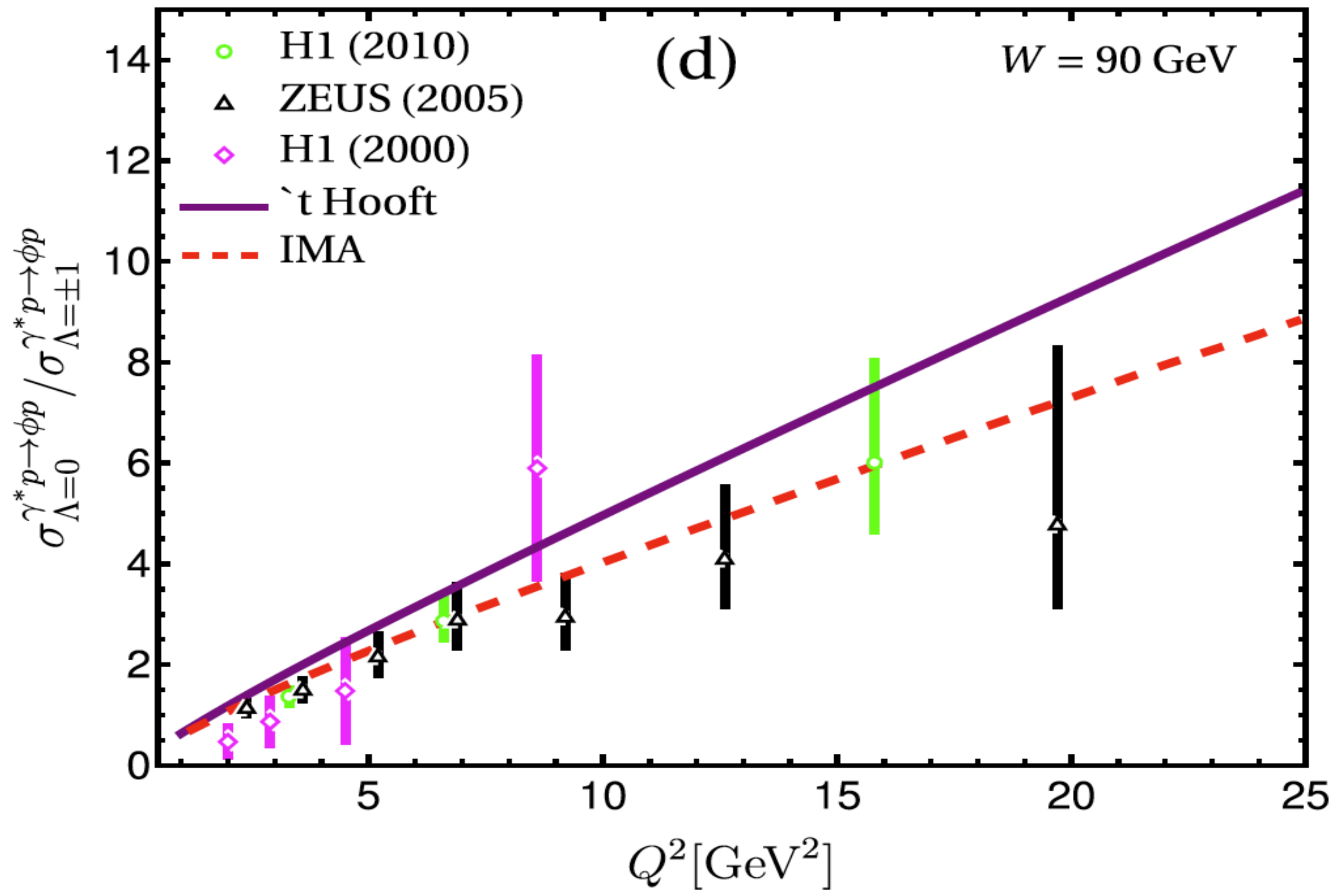

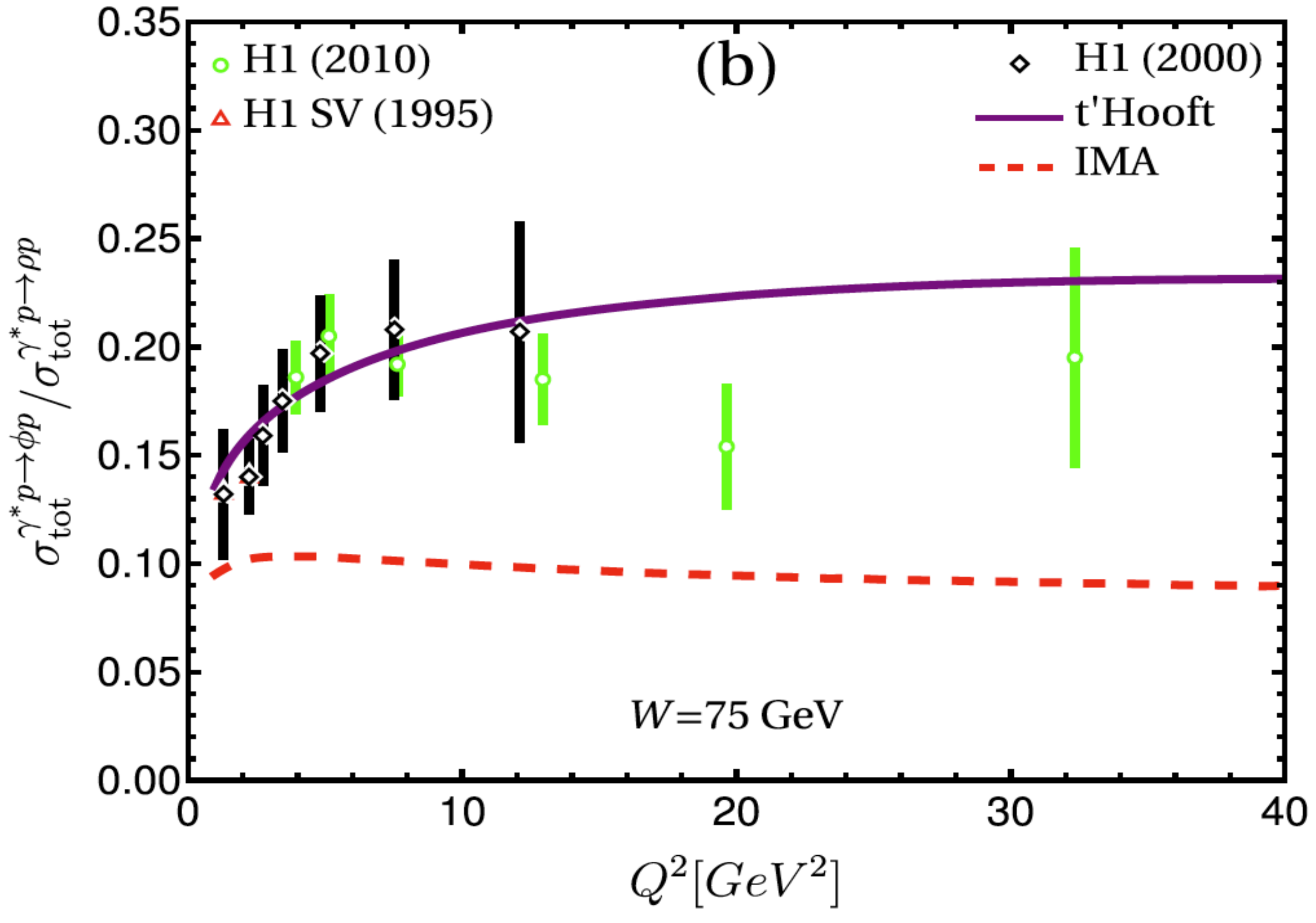

— BG, C. Mondal, S. Kaur, Phys.Rev.D 111 (2025)

J/ψ and $\psi(2S)$ - meson diffractive production

➡ HLFQCD and ’t-Hooft wave function for J/ψ meson

$$\Psi^{J/\psi,\lambda}_{\text{'t Hooft}}(r,x) = \mathcal{N}_\lambda x^\beta (1-x)^\beta \exp\left[-\frac{\kappa^2 x(1-x) r_\perp^2}{2}\right]$$

➡ wave function for $\psi(2S)$ → first radial excited state of J/ψ

$$\Psi^{\psi(2S),\lambda}_{\text{'t Hooft}}(r,x) = \mathcal{N}_\lambda x^\beta (1-x)^\beta \left(1 - \alpha\kappa^2 x(1-x) r_\perp^2\right) \times \exp\left[-\frac{\kappa^2 x(1-x) r_\perp^2}{2}\right],$$

➡ κ and β are fitted with electroproduction data from HERA and electronic decay width ($\chi^2/d.p = 0.60$)

$$\boxed{\kappa = 1.41,\ \beta = 4.62,\ \alpha = 0.74}$$

orthogonality conditions of mesonic states

➡ The polarization dependent normalization constant N_λ can be fixed through the normalization condition

$$\sum_{h,\bar{h}} \int \mathrm{d}^2\mathbf{r}\,\mathrm{d}x |\Psi^{V,\lambda}_{h,\bar{h}}(r,x)|^2 = 1.$$

— N. Sharma, PHYS. REV. D 109, 014019 (2024)

• Comparison with H1 and ZEUS data as a function of W for Q^2 bins

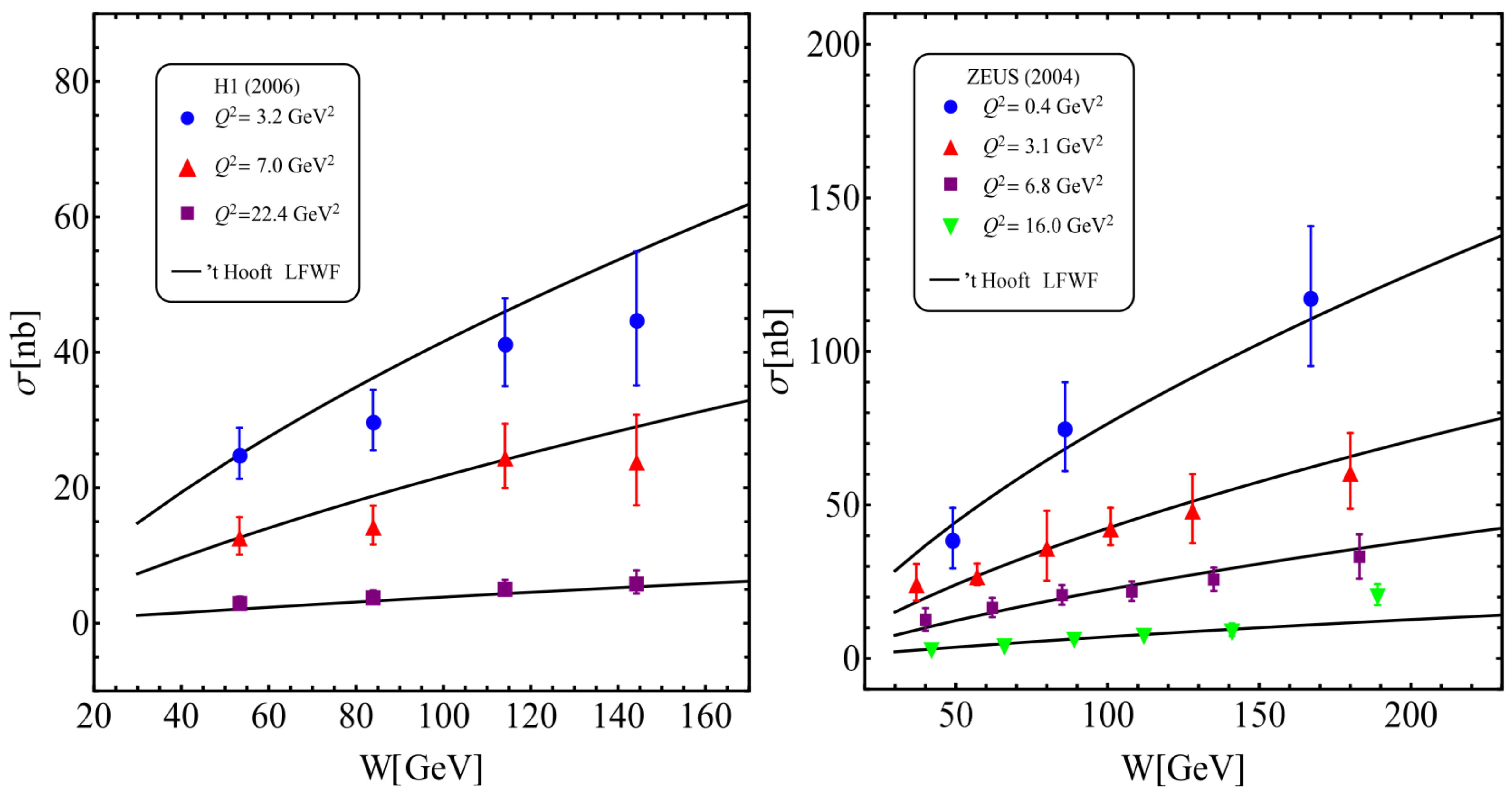

• Comparison with H1 and ZEUS data as a function of Q^2 at fixed W

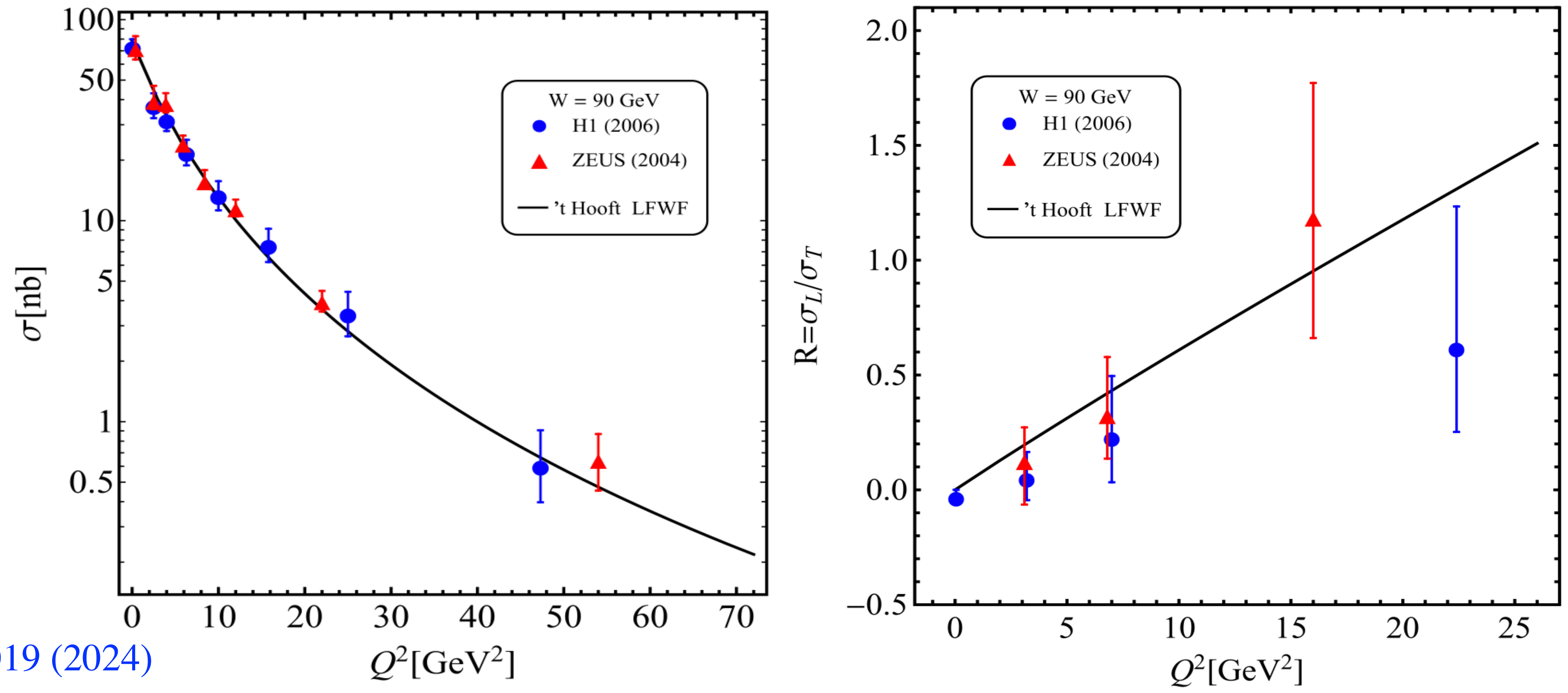

Rapidity distribution of VM production in UPC for $pp \to p \otimes V \otimes p$ process

- Comparison with H1 and ZEUS data as a function of $|t|$ for Q^2 bins at fixed W

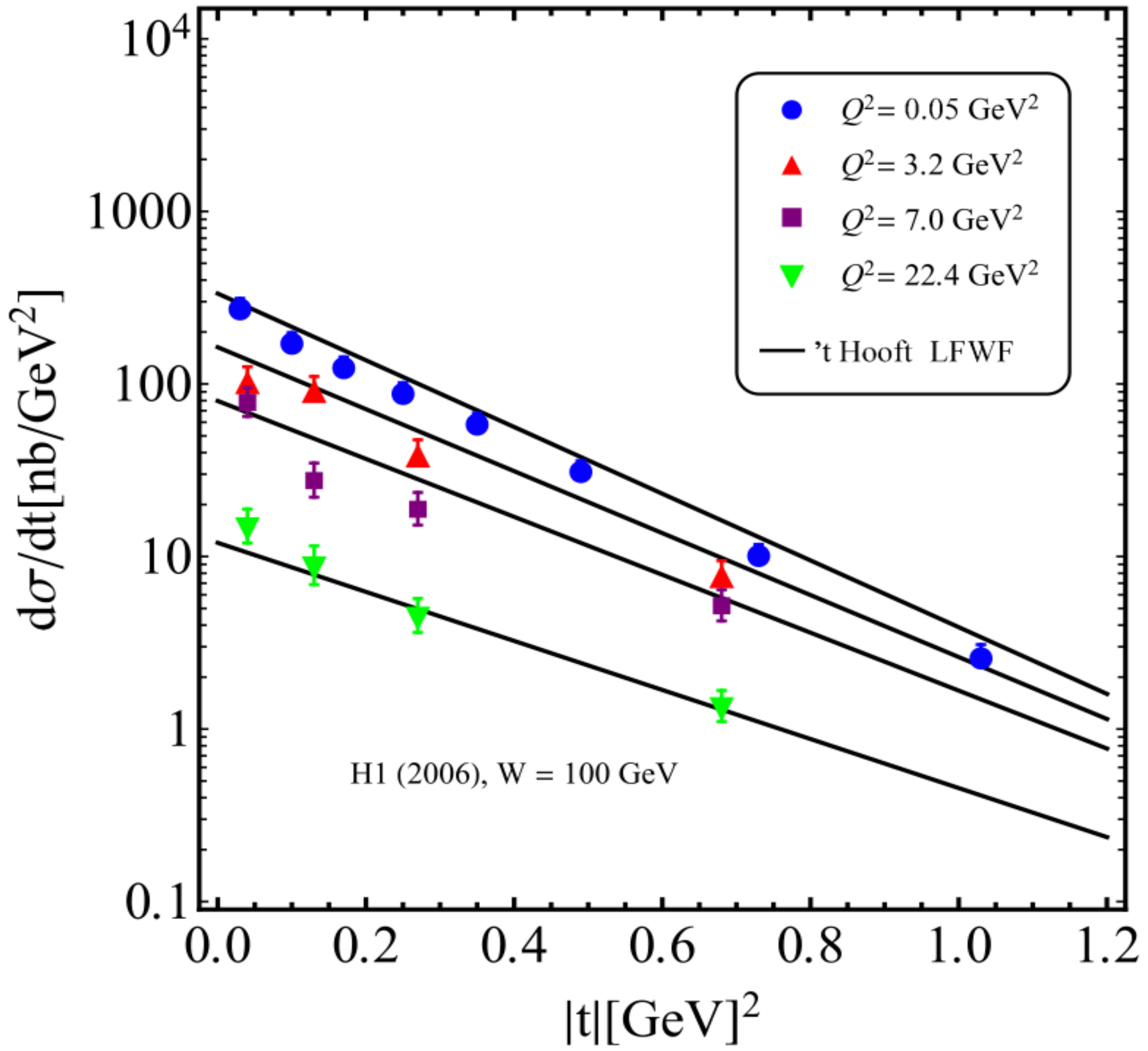

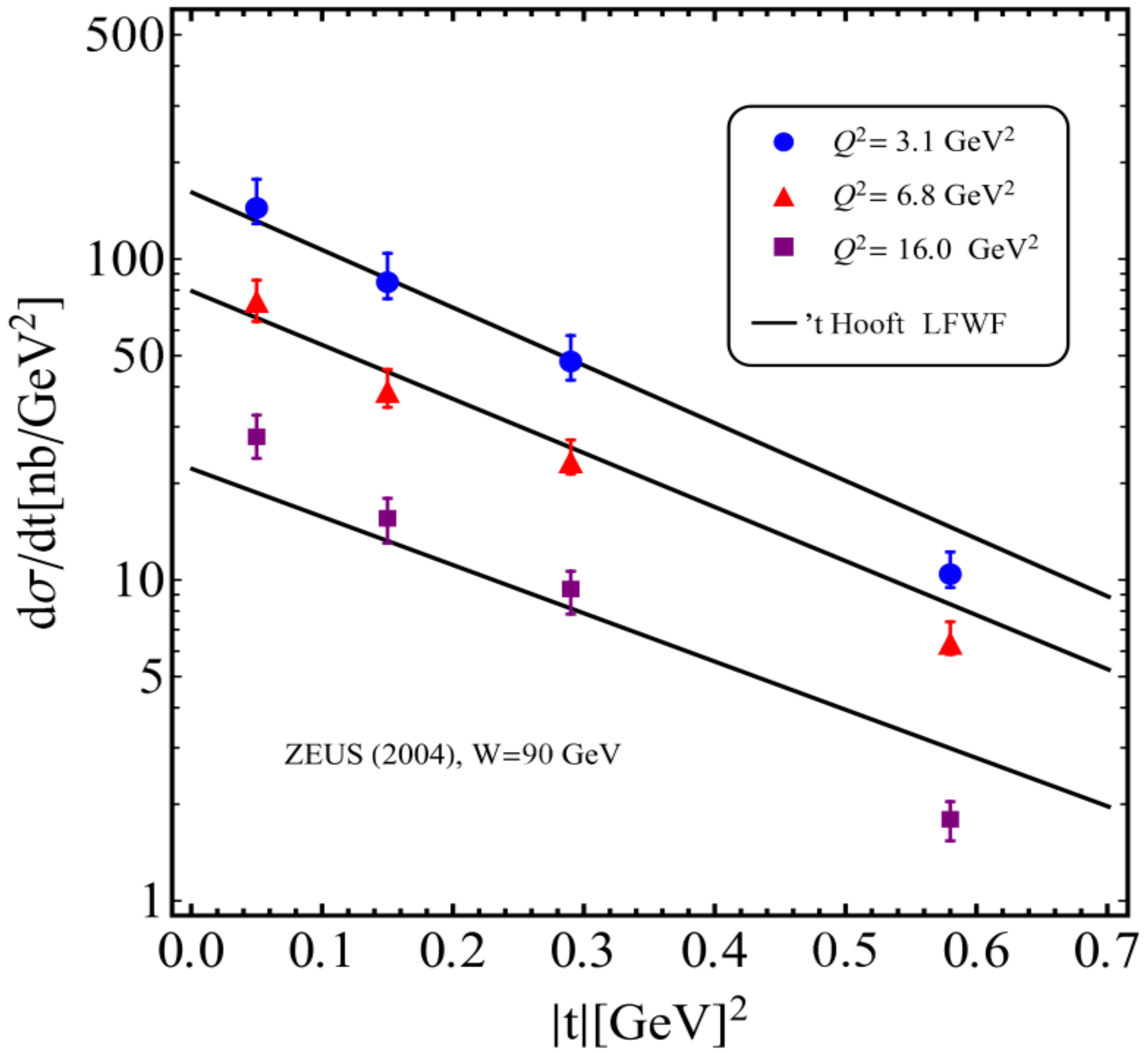

— N. Sharma, PHYS. REV. D 109, 014019 (2024)

➡ The differential cross section for the exclusive VM photoproduction off proton in pp UPCs

$$\frac{d\sigma[\mathrm{pp} \to \mathrm{p} \otimes J/\psi \otimes \mathrm{p}]}{dy} = S^2(W^+)\left(k^+\frac{\mathrm{dn}}{\mathrm{d}k^+}\right)\sigma^{\gamma p \to J/\psi p}(W^+) + S^2(W^-) \times \left(k^-\frac{\mathrm{dn}}{\mathrm{d}k^-}\right)\sigma^{\gamma p \to J/\psi p}(W^-),$$

— Jones, Martin, Ryskin, and Teubner, JHEP 11 (2013).

Photon momentum $\to$ $k^{\pm} = \frac{M_V}{2}\exp(\pm|\mathrm{y}|)$

Rapidity gap survival factors $\to S^2(W^{\pm})$

the photon flux

$$\frac{\mathrm{dn}}{\mathrm{dk}} = \frac{\alpha_{em}}{2\pi k}\left[1+\left(1-\frac{2k}{\sqrt{s}}\right)^2\right]\left(\ln\Omega - \frac{11}{6} + \frac{3}{\Omega} - \frac{3}{2\Omega^2} + \frac{1}{3\Omega^3}\right)$$

— Bertulani, Klein, and Nystrand, Annu. Rev. Nucl. Part. Sci. 55, 271 (2005).

$W^{\pm} = (2k^{\pm}\sqrt{s})^{1/2}$ $\to$ COM energy of the photon-proton system

- Comparison with LHCb data as a function of rapidity y for $\sqrt{s} = 7$, 13 TeV

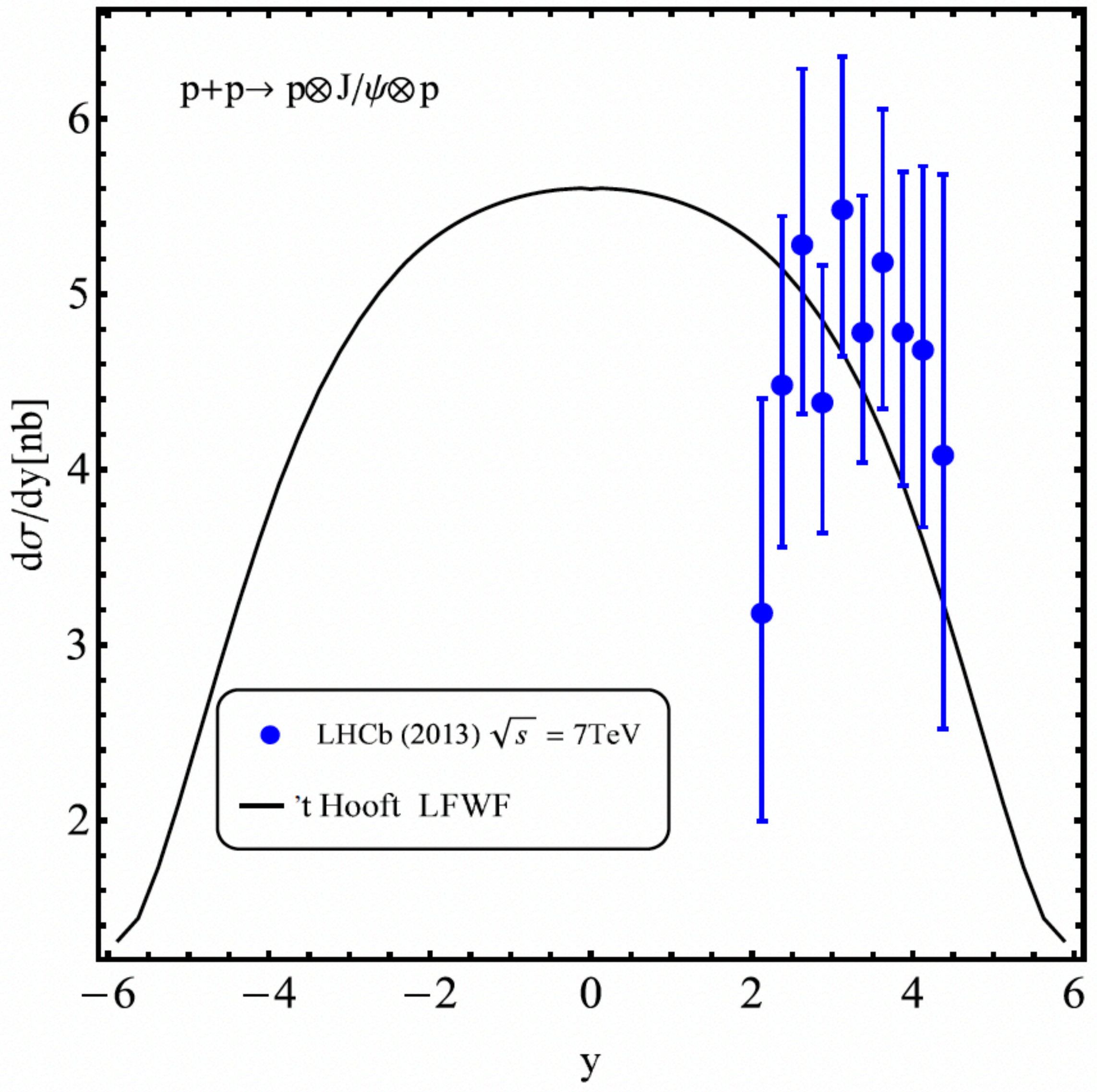

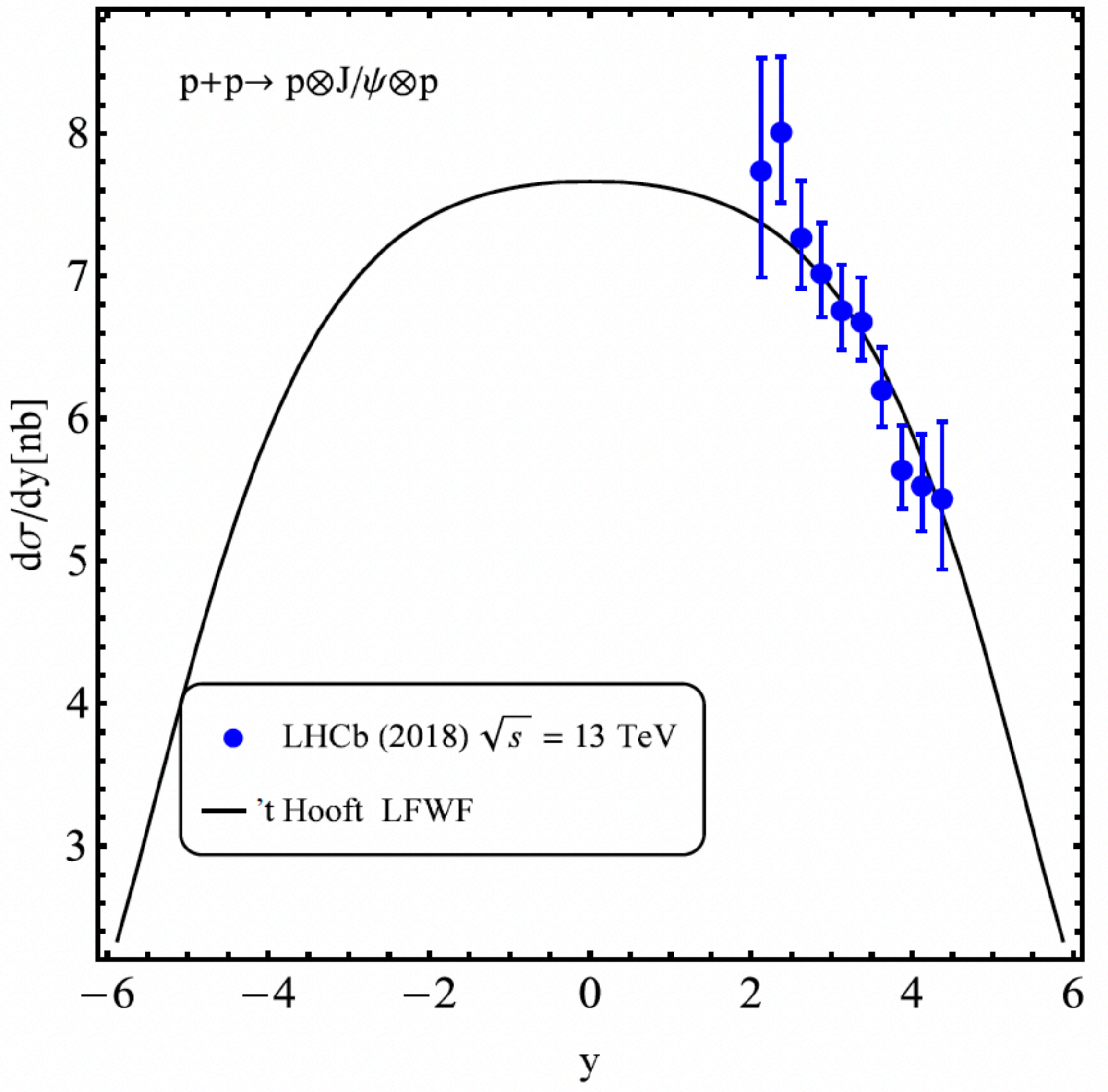

- Comparison with LHCb data as a function of rapidity y for $\sqrt{s} = 13$ TeV

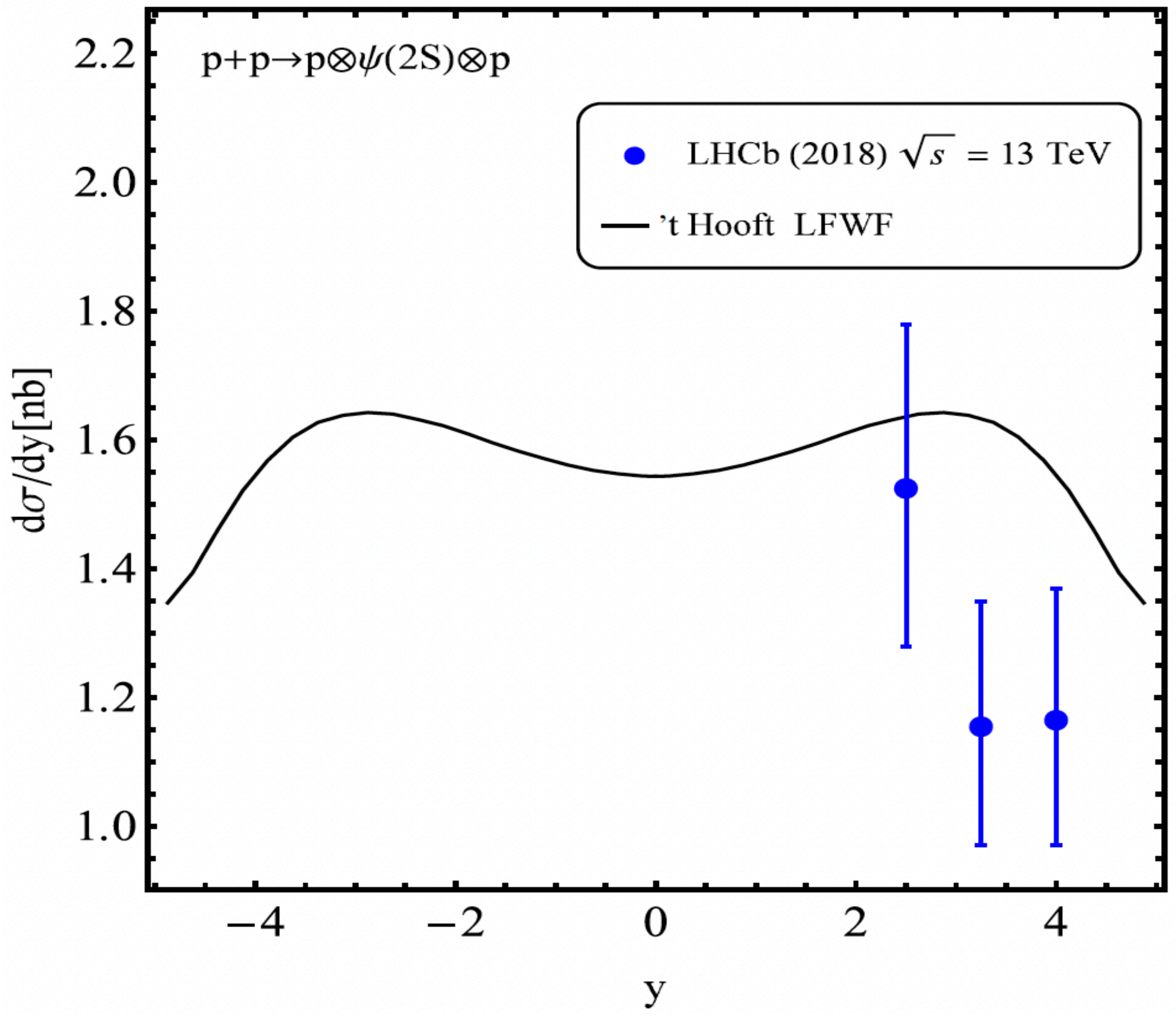

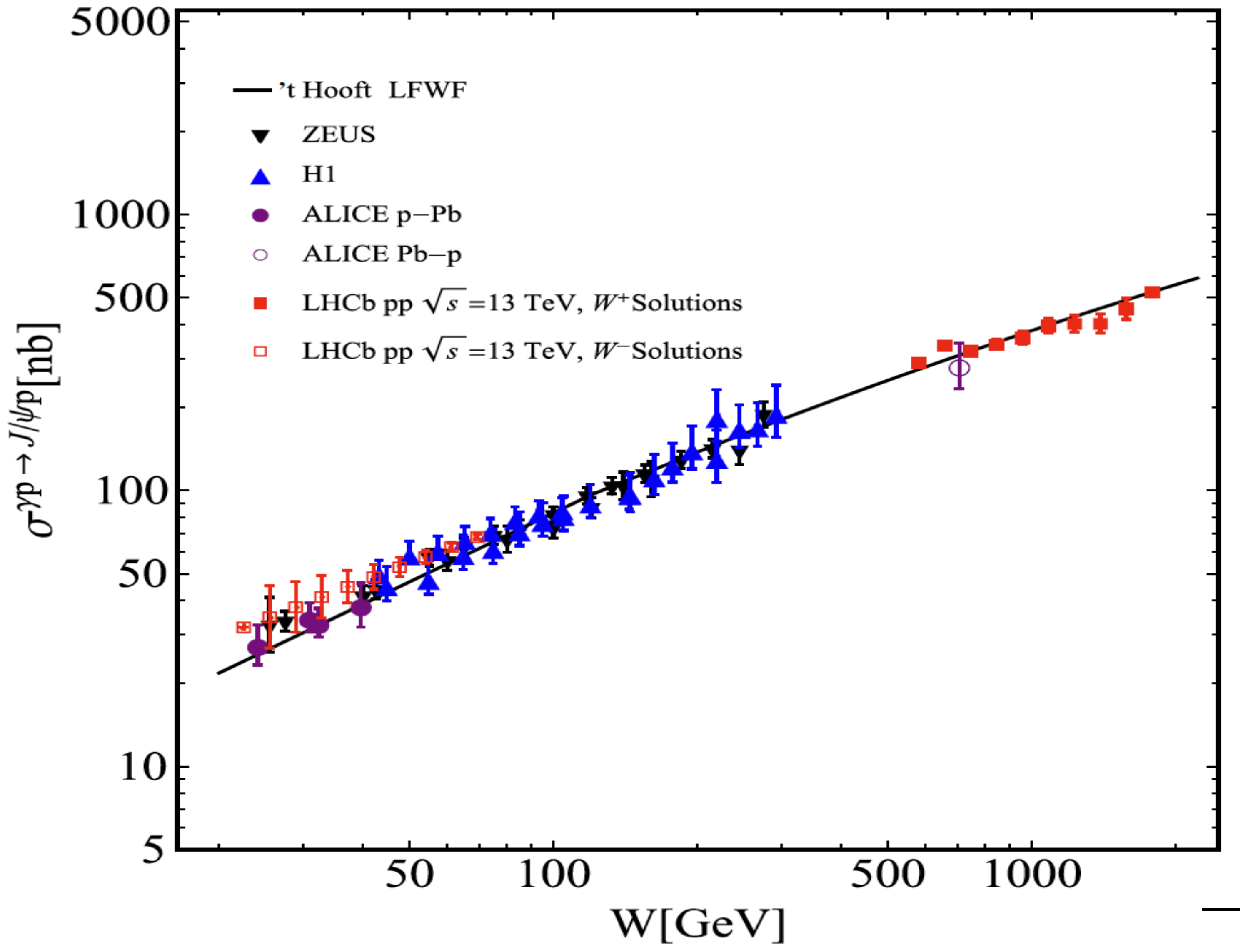

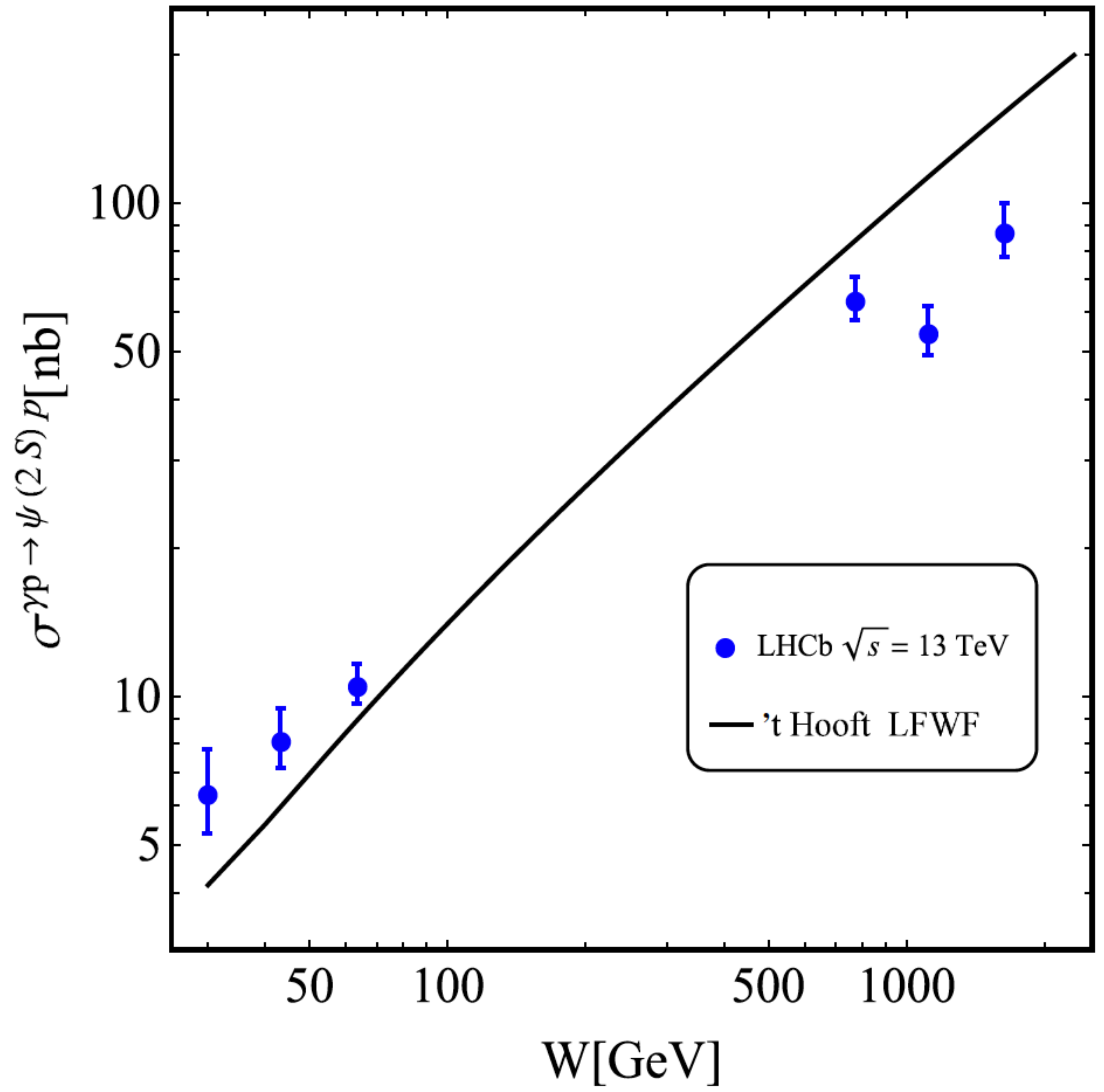

— N. Sharma, PHYS. REV. D 109, 014019 (2024)

- The ratio of $\psi(2S)$ to J/ψ photoproduction cross section as a function of W.

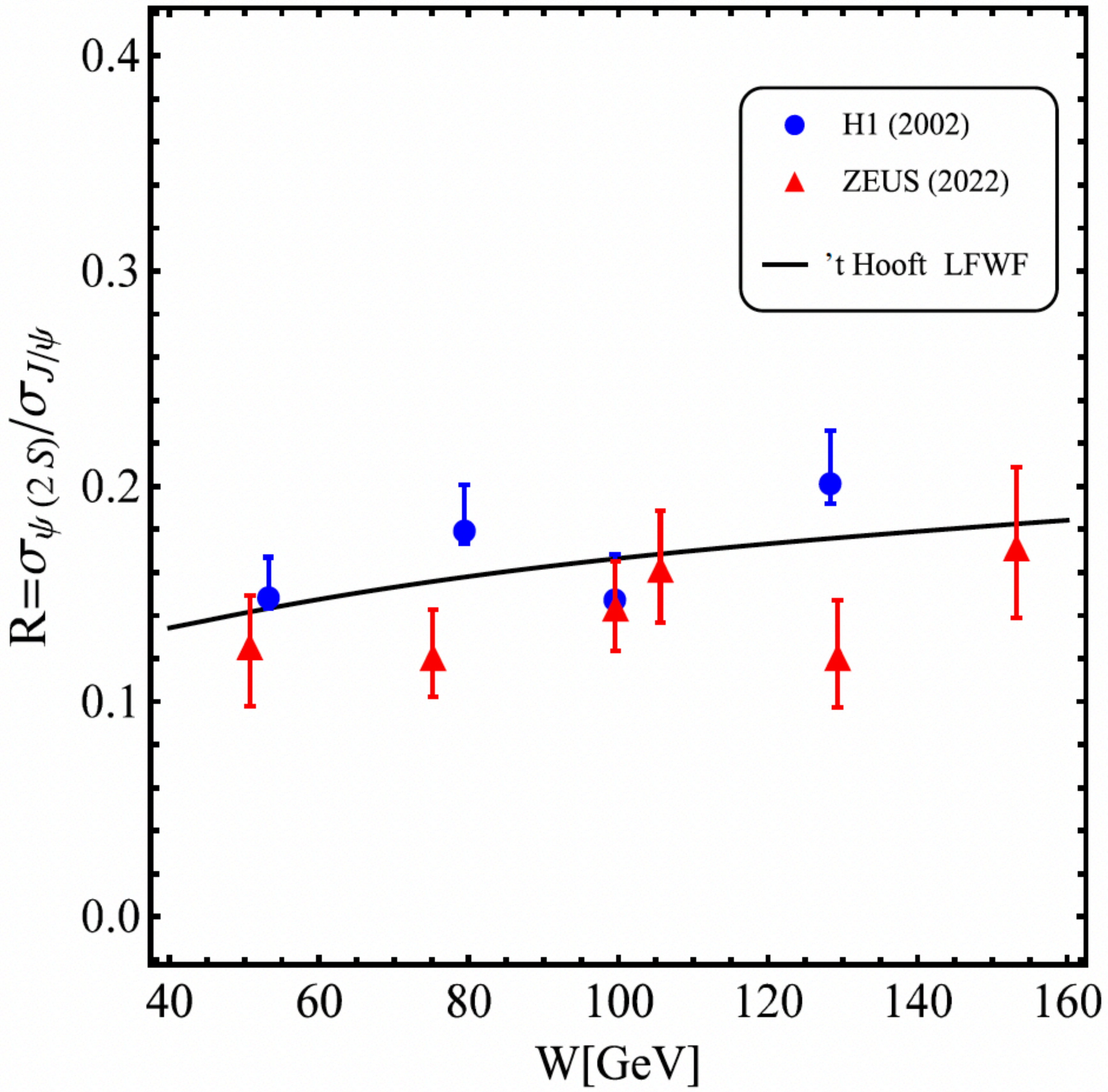

- The R value is very small signifying that the $\psi(2S)$ cross section is much suppressed than the J/ψ.
- The model predictions are in very good agreement with the experimental data for J/ψ.
- More data needed to check the consistency for $\psi(2S)$.

Exclusive and J/ψ photoproduction in $e\ A$ collisions

➡ eA collisions use the nuclear mass ($A^{1/3}$) to amplify gluon density, making saturation accessible at lower energies.

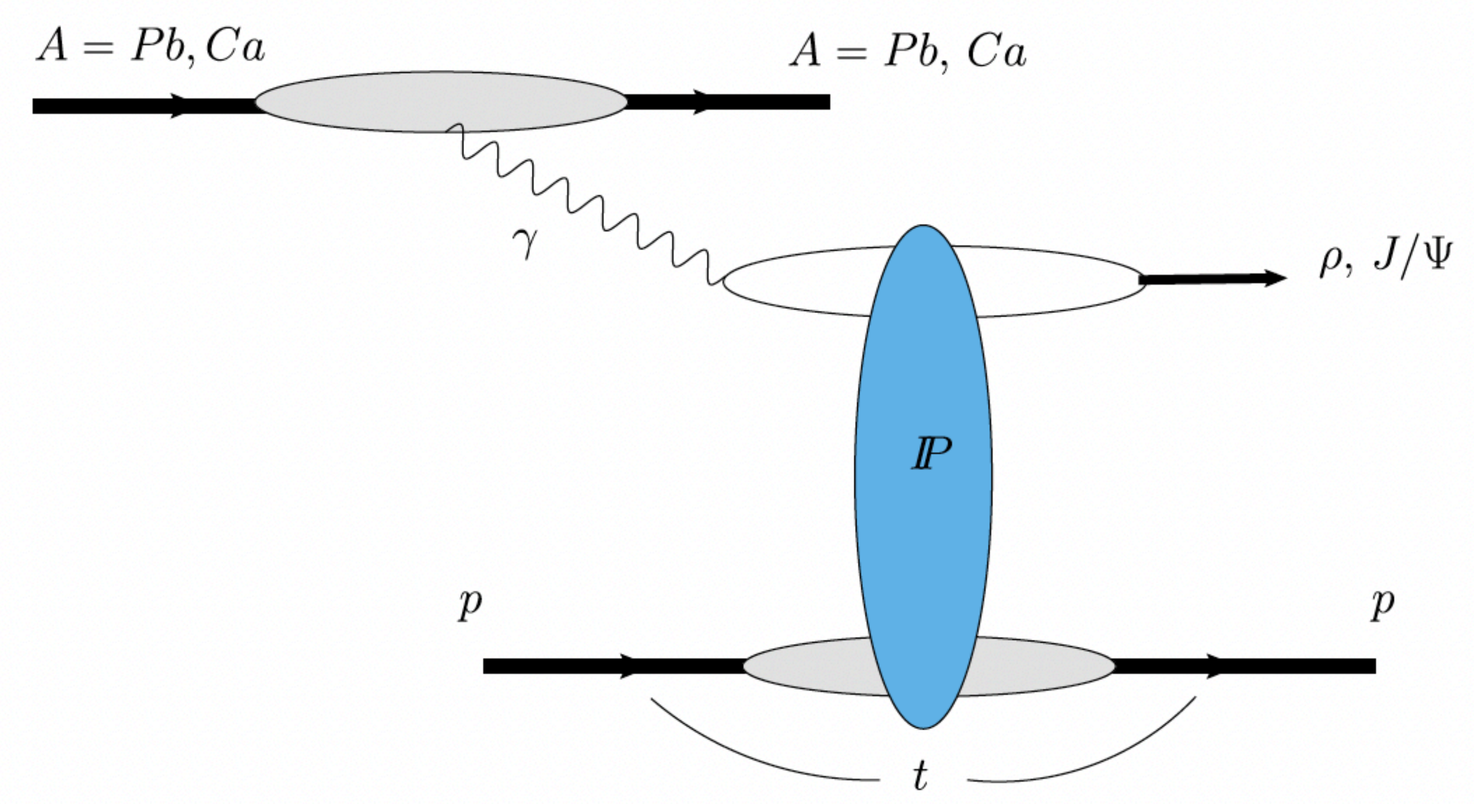

$$\frac{d\sigma\ [A+p \to A \otimes V \otimes p]}{dY\,dt} = n_A(\omega) \cdot \frac{d\sigma}{dt}(\gamma p \to V \otimes p)$$

➡ $\otimes$ represents the rapidity gap in the final state

- Rapidity → $\boxed{[Y \propto \ln(\omega/M_V)]}$
- $n_A(\omega)$ → equivalent photon spectrum of the relativistic incident nucleus.

$$n_A(\omega) = \frac{2Z^2\alpha_{em}}{\pi}\left[\xi K_0(\xi)K_1(\xi) - \frac{\xi^2}{2}\left(K_1^2(\xi) - K_0^2(\xi)\right)\right]$$

$$\boxed{Q_s^2(x) \sim A^{1/3}\left(\frac{1}{x}\right)^{\lambda}}$$

$$\lambda \sim 0.2 - 0.3$$

theoretical expectations for the saturation scale

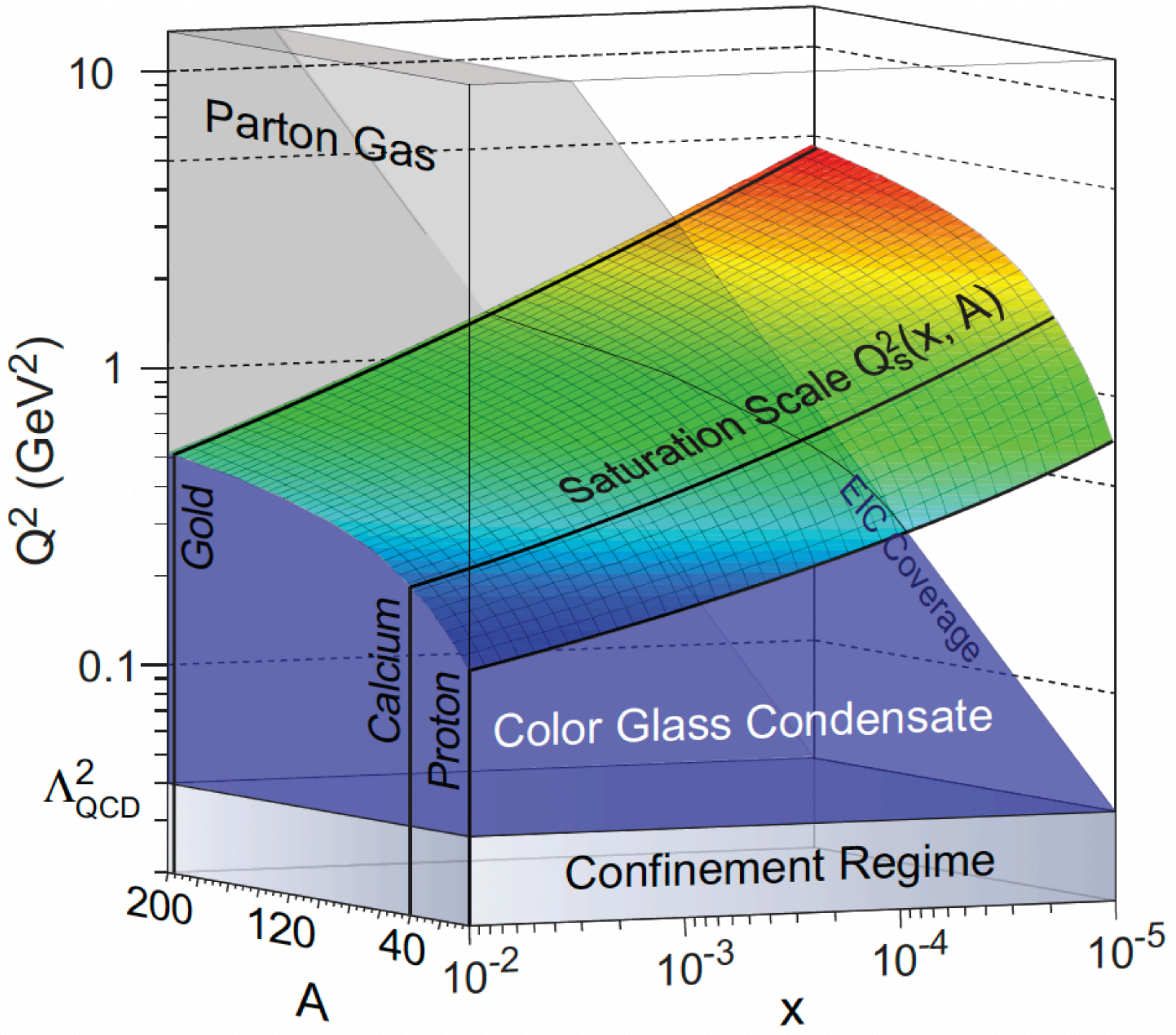

γ & J/ψ VM Wave function overlap

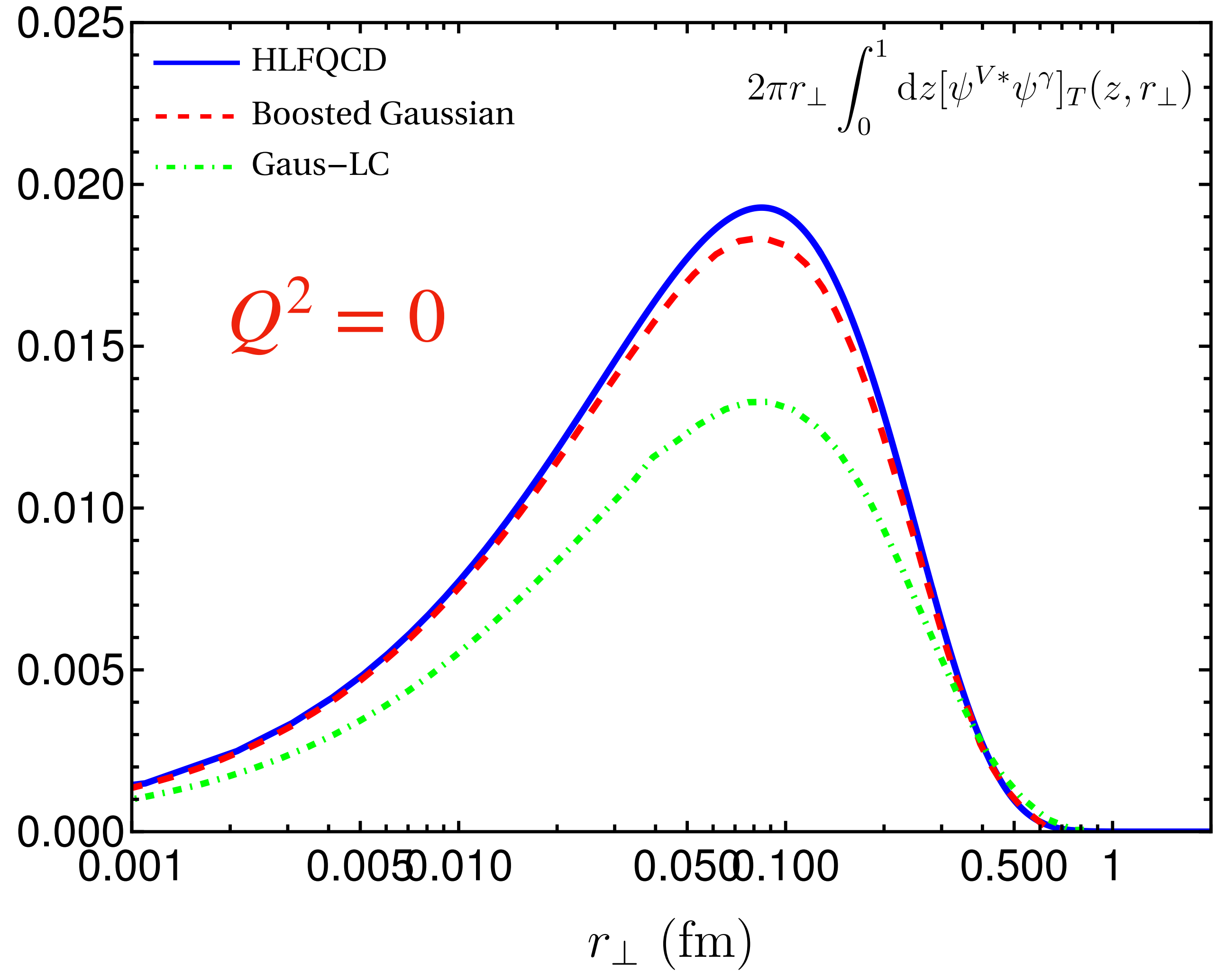

- HLFQCD wave function overlap is consistent with BG.

— Gonçalves, Navarra, Spiering , PLB 791 (2019),
— Bertulani, Baur, Phys. Rep. 163 (1988) 299,
— Kowalski and Teaney, PRD 68(2003).
— Gribov, Levin, and Ryskin, Phys. Rept. (1983).

Preliminary results for J/ψ photoproduction in eA collision

➡ The differential cross sections for the exclusive photoproduction as a function of $|t|$ at three different values for the vector meson rapidity.

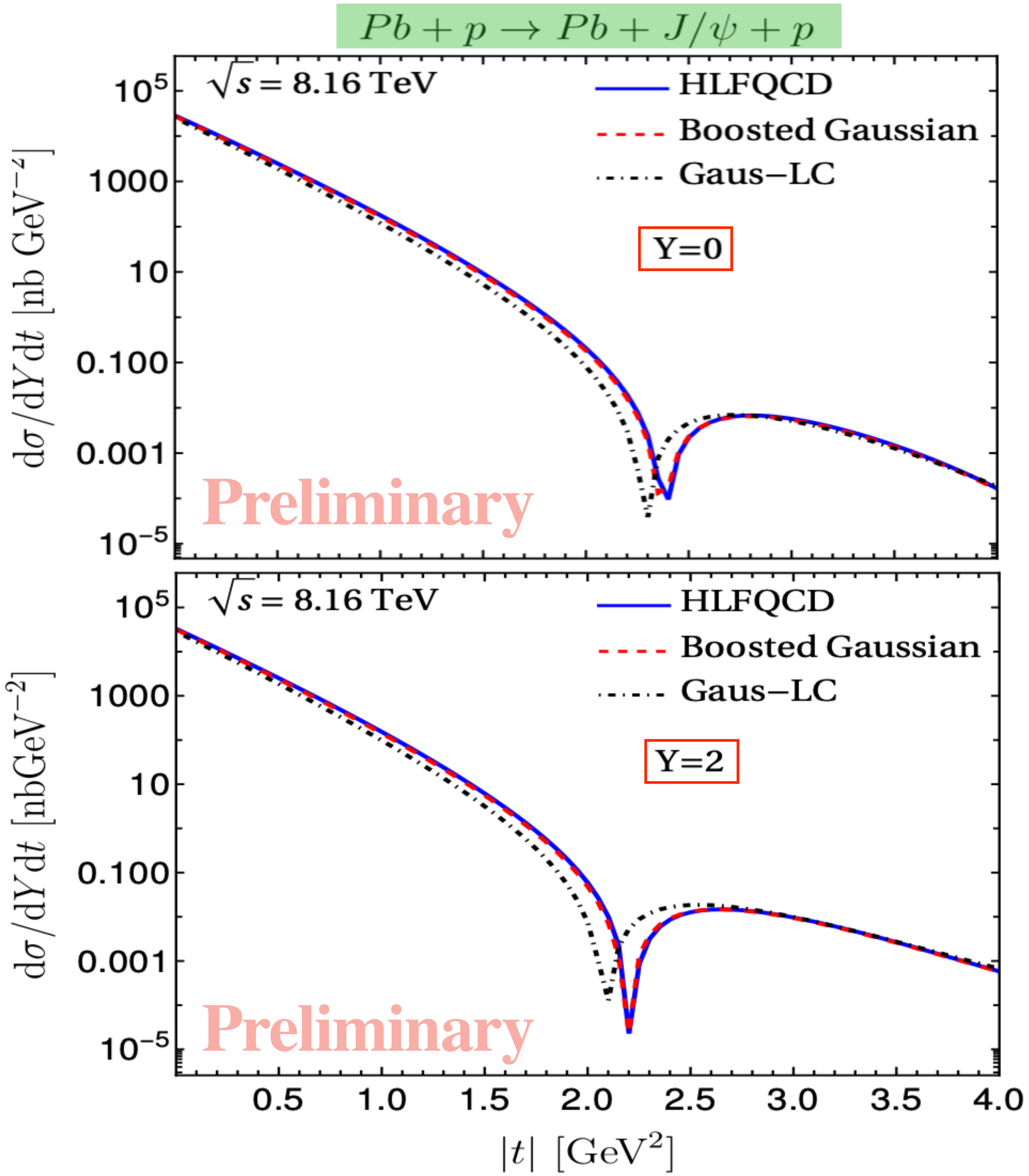

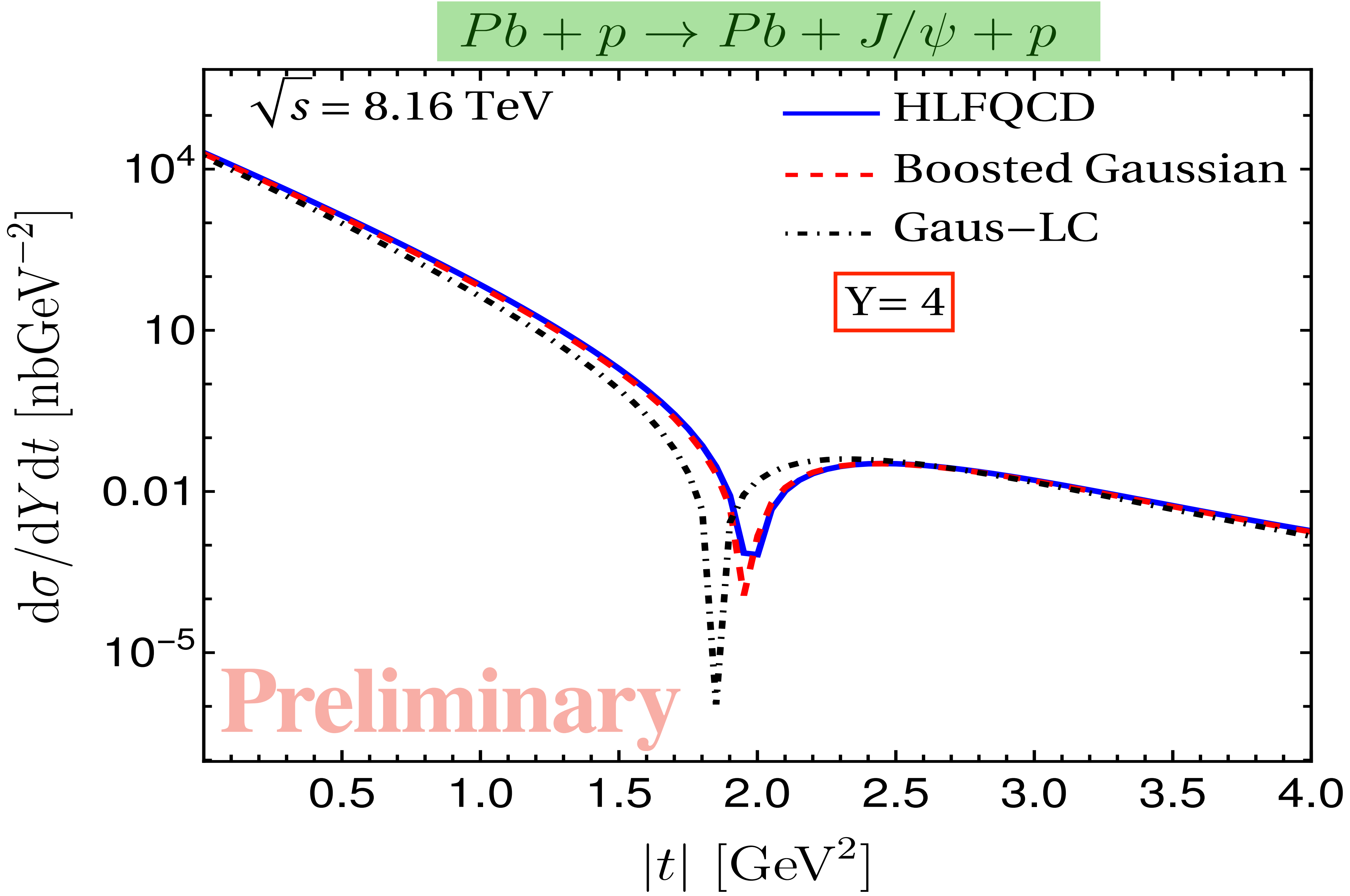

➡ Rapidity distribution of J/ψ photoproduction from Ca and Pb and compared with BG and GLC wave functions.

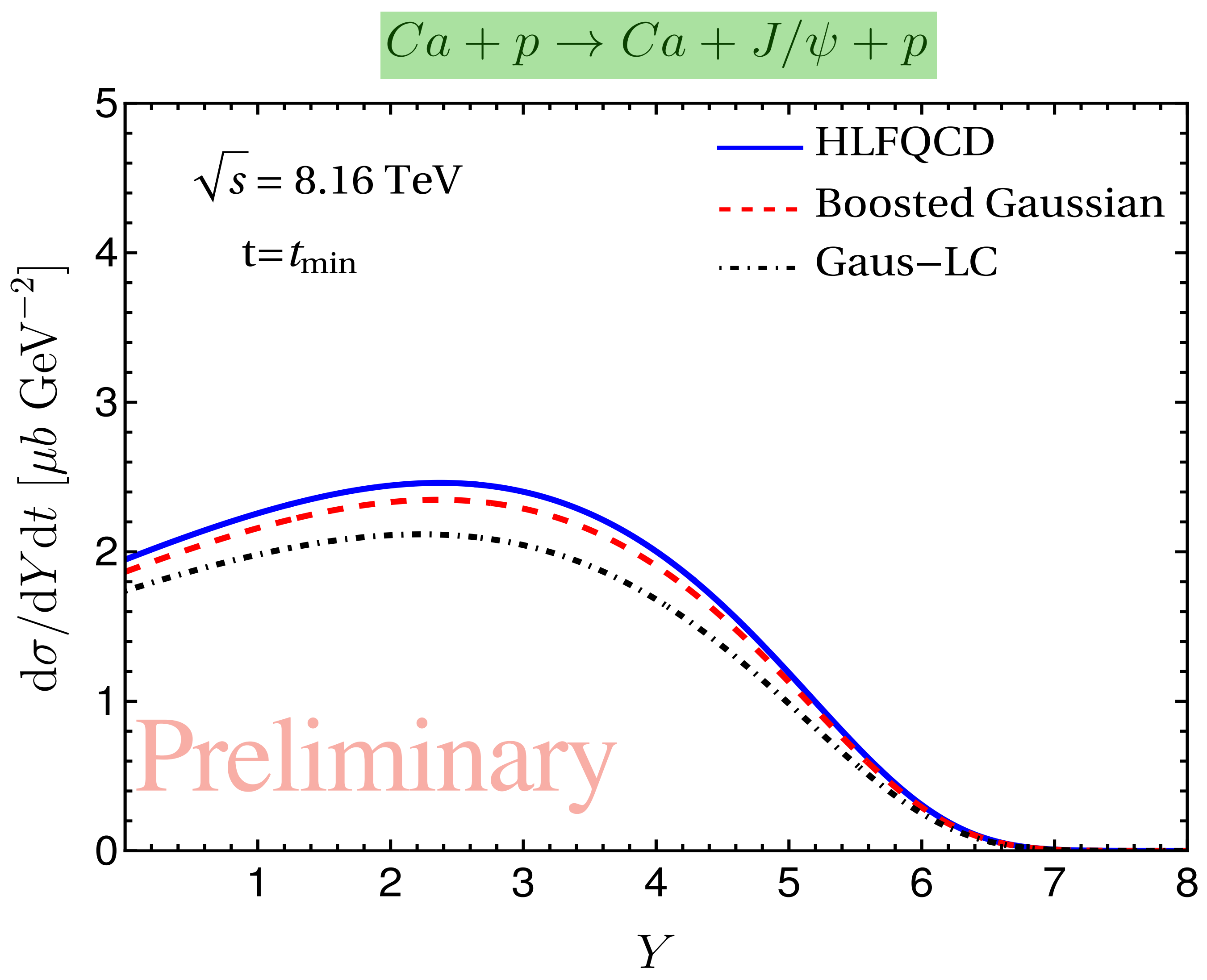

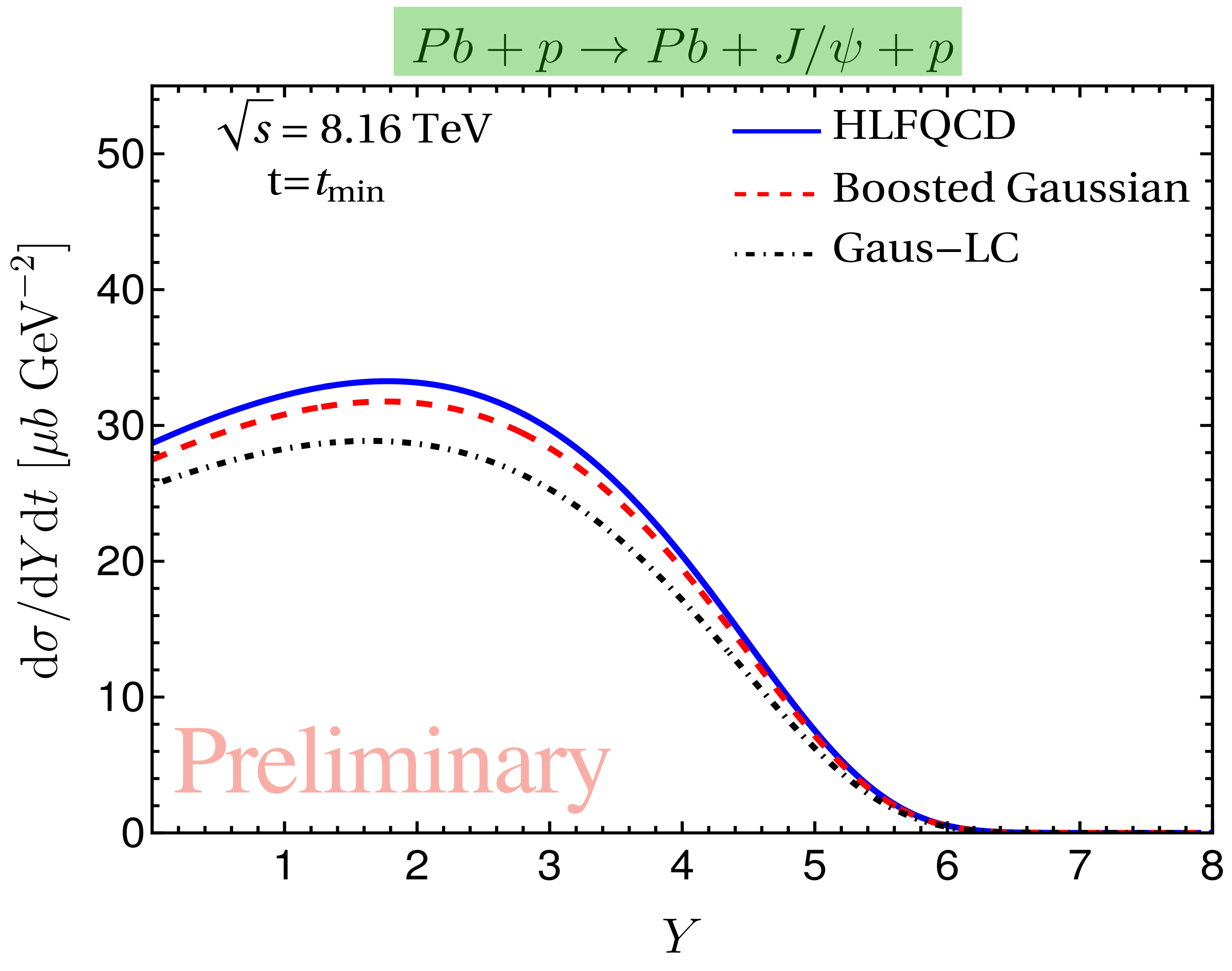

Conclusion & Outlook

- Color glass condensate (CGC) is a theoretical framework widely used to explain physical phenomena occurring within proton saturation region.
- Light-front QCD is a natural framework to describe hadrons as relativistic bound states.
- Holographic Light-Front QCD (HLFQCD) predictions along with ‘t Hooft equation for diffractive $\rho, \phi, J/\psi$ and production are in good agreement with the HERA data.
- The ϕ to ρ total cross section ratios are found to be independent of $(Q^2 + M_v^2)$ and consistent with ratio expected from quark charge counting, $\phi : \rho = 2 : 9$.
- The incoherent electro and photoproduction is crucial to probe the gluon density fluctuations inside the target.
- EIC is a unique opportunity to complete the discovery of saturation/CGC physics and to study its properties.

Thanks for your attention !!

Questions ??